Initiation and Frequency of Debris Flows in Grand Canyon, Arizona

U.S. GEOLOGICAL SURVEY
Open-File Report 96—491

Prepared in cooperation with the
BUREAU OF RECLAMATION

Initiation and Frequency of Debris Flows in Grand Canyon, Arizona

By PETER G. GRIFFITHS, ROBERT H. WEBB, and THEODORE S. MELIS

U.S. GEOLOGICAL SURVEY
Open-File Report 96—491

Prepared in cooperation with the
BUREAU OF RECLAMATION

Tucson, Arizona
1996

U.S. DEPARTMENT OF THE INTERIOR
BRUCE BABBITT, Secretary

U.S. GEOLOGICAL SURVEY
Gordon P. Eaton, Director

For additional information
write to:

Regional Research Hydrologist
U.S. Geological Survey, MS-472
Water Resources Division
345 Middlefield Road
Menlo Park, CA 94025

Copies of this report can be
purchased from:

U.S. Geological Survey
Branch of Information Services
Box 25286
Denver, CO 80225

CONTENTS

	Page
Abstract	1
Introduction	2
Purpose and Scope	3
Units and Place Names	3
Acknowledgments	5
Setting	5
Methods	7
Initiation Mechanisms and Precipitation Recurrence Intervals	7
Selection of Geomorphically Significant Tributaries	7
Repeat Photography and Binomial Frequency of Debris Flows	8
Morphometric, Lithologic, and Climatic Variables	10
Statistical Procedures	13
Initiation of debris flows	15
Importance of Shale	21
Logistic-Regression Analyses	23
Eastern Grand Canyon	23
Western Grand Canyon	26
Non-Significant Variables	27
Discussion and Conclusions	32
References Cited	33

FIGURES

1. Map showing the Colorado River in Grand Canyon National Park, Arizona 3
2. Diagram showing the morphology of a typical debris fan in Grand Canyon 4
3. Stratigraphic column showing rocks exposed in Grand Canyon 6
4. Replicate photographs showing the debris fan at Ruby Rapid in Grand Canyon 8
5. Replicate photographs showing the debris fan at South Canyon in Marble Canyon 10
6. Histograms showing the statistical distributions of tributary drainage areas in Grand Canyon 14
7. Map of Grand Canyon showing tributaries with debris-flow histories 16
8. Photograph showing debris-flow source areas in Monument Creek 18
9. Graph showing the failure mechanisms that have initiated debris flows in Grand Canyon 19
10. Schematic diagram illustrating the initiation of debris flows by the direct failure of bedrock in Grand Canyon 19
11. Photograph showing colluvial wedges overlying Muav Limestone 22
12. Schematic diagram illustrating the initiation of debris flows by failure of colluvial wedges during rainfall 23
13. Particle-size distribution of a debris-flow deposit 24
14. Graph showing the principal component scores of variables used in the logistic-regression analyses for eastern Grand Canyon 26
15. Graph showing the relation between drainage area and gradient in western Grand Canyon 29
16. Graph showing the principal component scores of variables used in the logistic-regression analyses for western Grand Canyon 29
17. Graph showing the relation between drainage area and gradient in eastern Grand Canyon 30
18. Map showing the probability of debris flows in tributaries of the Colorado River in Grand Canyon 31
19. Histograms of the probability of debris-flow occurrence in eastern and western Grand Canyon . 32

TABLES

Page

1. Mean annual precipitation and temperatures in the vicinity of Grand Canyon 7
2. Drainage-basin variables used in logistic regression 12
3. Precipitation associated with selected debris flows in Grand Canyon 17
4. Clay mineralogy of source material and debris flows in Grand Canyon 25
5. Calibration model for debris-flow probability in tributaries of eastern Grand Canyon 28
6. Verification model for debris-flow probability in tributaries of eastern Grand Canyon 28
7. Calibration model for debris-flow probability in tributaries of western Grand Canyon 28
8. Verification model for debris-flow probability in tributaries of western Grand Canyon 30

CONVERSION FACTORS

For readers who prefer to use inch-pound units, conversion factors for the terms in this report are listed below:

Multiply	By	To obtain
millimeter (mm)	0.03937	inch (in.)
meter (m)	3.2818	foot (ft)
square meter (m^2)	10.76	square foot (ft^2)
kilometer (km)	0.6214	mile (mi)
square kilometer (km^2)	0.3861	square mile (mi^2)

Sea level: In this report, “sea level” refers to the National Geodetic Vertical Datum of 1929 (NGVD of 1929)--a geodetic datum derived from a general adjustment of the first-order level nets of both the United States and Canada, formerly called “Sea Level Datum of 1929.”

Initiation And Frequency Of Debris Flows In Grand Canyon, Arizona

By Peter G. Griffiths, Robert H. Webb, and Theodore S. Melis

ABSTRACT

Debris flows occur in 600 tributaries of the Colorado River in Grand Canyon, Arizona when intense precipitation causes slope failures in bedrock or colluvium. These slurries transport poorly sorted sediment, including very large boulders that form rapids at the mouths of tributaries and control the longitudinal profile of the Colorado River. Although the amount of rainfall on the days of historic debris flows typically is not unusual, the storm rainfall on consecutive days before the debris flows typically had recurrence intervals greater than 10 yrs. Four types of failure mechanisms initiate debris flows: bedrock failure (12 percent), failure of colluvial wedges by rainfall (21 percent), failure of colluvial wedges by runoff (the "firehose effect;" 36 percent), and combinations of these failure mechanisms (30 percent). Failure points are directly or indirectly associated with terrestrial shales, particularly the Permian Hermit Shale, shale units within the Permian Esplanade Sandstone of the Supai Group, and the Cambrian Bright Angel Shale. Shales either directly fail, produce colluvial wedges downslope that contain clay, or form benches that store poorly sorted colluvium in wedge-shaped deposits. Terrestrial shales provide the fine particles and clay minerals — particularly kaolinite and illite — essential to long-distance debris-flow transport, whereas marine shales mostly contain smectites, which inhibit debris-flow initiation.

Using repeat photography, we determined whether or not a debris flow occurred in the last century in 164 of 600 tributaries in Grand Canyon. We used logistic regression to model the binomial frequency data using 21 morphometric and lithologic variables. The location of shale units, particularly the Hermit Shale, within the tributary is the most consistent variable related to debris-flow frequency in Grand Canyon. Other statistically significant variables vary with large scale changes in canyon morphology. Standard morphometric measures such as drainage-basin area, channel gradient, and aspect of the river corridor are the most significant variables in the narrow and deep eastern section of Grand Canyon. Measures of the location of source lithologies are more important in western Grand Canyon, which has broader and low-gradient drainages. Measures of geologic structure, and other standard hydrologic variates, were not significant.

Our results show that the probability of debris-flow occurrence is highest in eastern Grand Canyon. Throughout Grand Canyon, the probability of debris-flow occurrence is highest in reaches of the Colorado River that trend south-southwest. This direction is significant because most summer storms originate from a southerly direction, and the maximum slope of the regional structure is to the southwest. The binomial frequency of debris flows is not random in Grand Canyon, and tributaries of similar debris-flow frequency are clustered in distinct reaches.

INTRODUCTION

Debris flows are the primary sediment transport process in 600 tributaries of the Colorado River between Lees Ferry and Diamond Creek, Arizona (fig. 1). This type of flash flood contains up to 80 percent sediment by weight and deposits poorly sorted sediment that ranges from fine clays to extremely large boulders (b-axis > 3 m) in the river (Melis and others, 1994). All but the largest boulders were entrained by typical, pre-dam Colorado River floods, and debris fans, which are composed of residual boulders, form rapids in the Colorado River (fig. 2). Because debris fans raise the bed elevation (Howard and Dolan, 1981), the Colorado River forms large pools upstream from rapids. Flow through rapids ends in pools (Dolan and others, 1978; Kieffer, 1985), the downstream end of which is controlled by bedrock outcrops or alternating debris bars that are outwash from the upstream debris fan (Howard and Dolan, 1981; Webb and others, 1989; Melis and Webb, 1993; Melis and others, 1994). Half of the vertical drop of the Colorado River occurs in rapids, which account for only 10 percent of the river's length through Grand Canyon (Leopold, 1969). By forming rapids, debris flows define the longitudinal profile and control the geomorphic framework of the Colorado River in Grand Canyon (Webb, 1996).

A better understanding of the factors and processes involved in the initiation of debris flows is critical to understanding the dynamic processes that shape and control the Colorado River in Grand Canyon National Park. Moreover, debris flows are a significant geomorphic hazard worldwide (Costa and Wieczorek, 1987). The debris-flow process is of interest not only to scientists but also to the more than 20,000 whitewater enthusiasts that run the rapids in Grand Canyon every summer (Stevens, 1990). An average-sized debris flow can alter the severity of a major rapid or riffle, or cover a popular camping beach with boulder-strewn debris in a matter of seconds. Because of operation of Glen Canyon Dam, rapids constricted by debris flows are only partially reworked by flow in the regulated Colorado River (Graf, 1980; Melis and Webb, 1993; Webb and others, 1996).

Most of Grand Canyon is unaffected by humans and provides an excellent setting for studying debris-flow processes that are little influenced by land-use practices. Also, the scenic beauty of Grand Canyon has generated an enormous body of photographs of the Colorado River beginning in 1872 (Melis and others, 1994). These photographs contain a wealth of information on the occurrence of debris flows over the last century (Webb, 1996), and provide us with binomial-frequency data: whether or not a debris flow has occurred in the last century.

This study examines the process of debris-flow initiation and transport in Grand Canyon and presents field observations on the roles of climate, canyon lithology, geologic structure, and drainage-basin morphometrics. Particular emphasis is given to the roles of intense precipitation and source areas. We evaluated the relative importance of different types of independent drainage-basin variables in generating debris flows using logistic regression (Hosmer and Lemeshow, 1989). Logistic-regression modeling permits the identification of statistically significant drainage-basin variables, isolating those geomorphic factors that most strongly control debris-flow initiation in the near-vertical cliffs of Grand Canyon and transport to the Colorado River.

The occurrence of debris flows in the last century was determined for 164 tributaries (the "calibration set") using repeat photography and analysis of hundreds of historical photographs taken of the river corridor from 1872 through 1995. Frequency information for 50 additional tributaries (the "verification set") was used to test the robustness of the logistic-regression model. Whether or not a debris flow occurred in that period was determined by analyzing the differences between historical photographs and the modern matches. We increased the available data (Melis and others, 1994) from 529 to 600 tributaries of the Colorado River by adding tributaries downstream from Diamond Creek for which frequency information is available. Using the model coefficients obtained from the calibration set, we estimated the probability of debris-flow occurrence for all 600 tributaries.

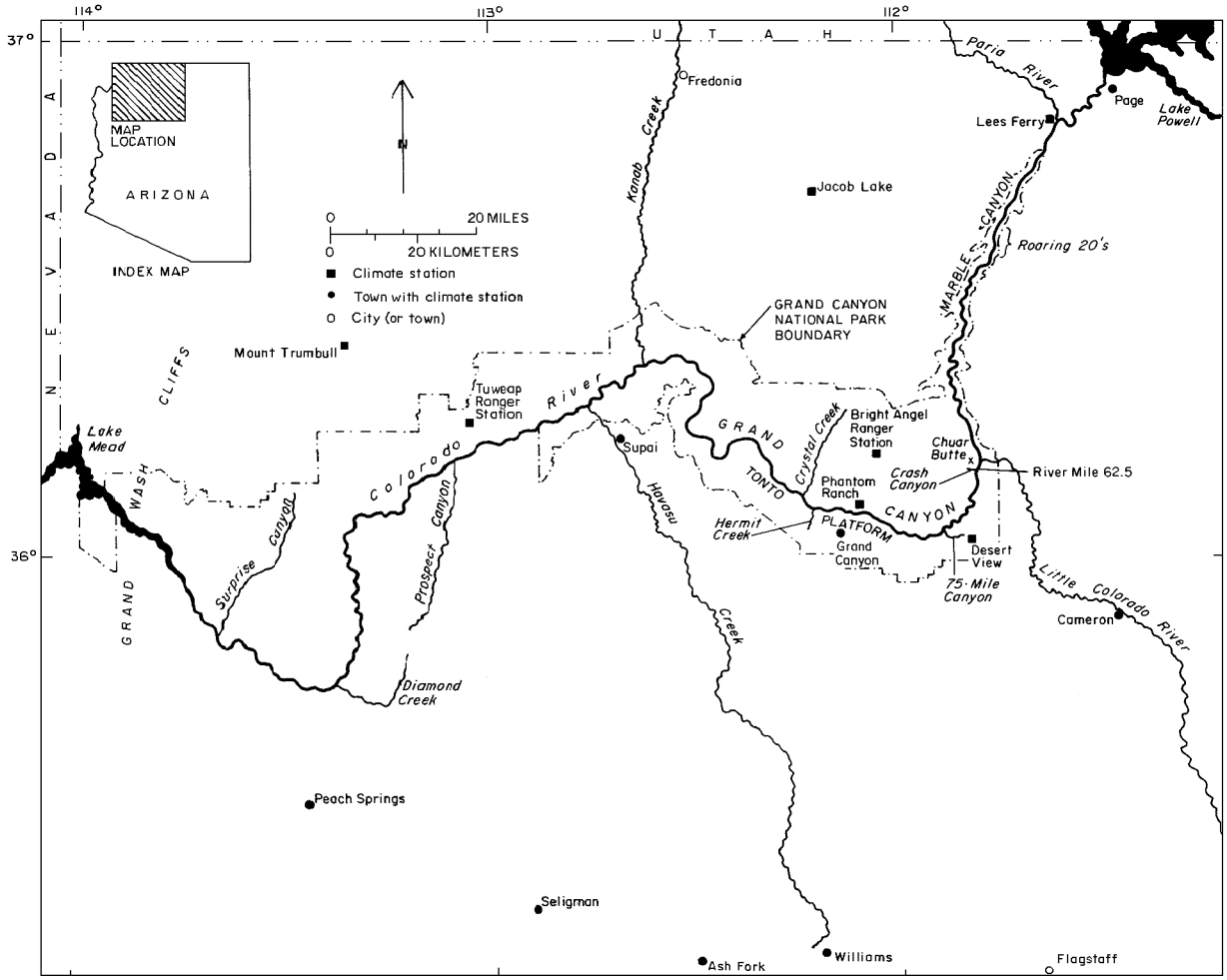

Figure 1. The Colorado River in Grand Canyon, Arizona.

Purpose and Scope

This study provides an analysis of initiation mechanisms and frequency of historic debris flows in Grand Canyon National Park and vicinity, Arizona. The data presented here will be used as the basis for development of sediment-yield estimates from ungaged tributaries of the Colorado River, a critical element of long-term management of resources downstream from Glen Canyon Dam (U.S. Department of Interior, 1995). This report incorporates existing information on debris-flow frequency in Grand Canyon (Cooley and others, 1977; Webb and others, 1989; Melis and others, 1994), and includes 600 tributaries of the Colorado River between Lees Ferry and Surprise Canyon, Arizona (river miles 0 to 248), excluding the Paria and Little Colorado Rivers and Kanab and Havasu Creeks. Repeat photography from the 1889-1890 Stanton expedition (Webb, 1996) provides uniform data for estimation of the binomial frequency of debris flows in 164 tributaries in Grand Canyon. Logistic regression is used to develop a statistical model based on measured morphometric, lithologic, and climatic variables from these 164 tributaries for estimation of the probability of debris-flow occurrence in all 600 geomorphically significant tributaries. This work was funded in cooperation with the Glen Canyon Environmental Studies Program of the Bureau of Reclamation.

Units and Place Names

In this report, we use the inch-pound unit of mile to describe location of tributaries along the

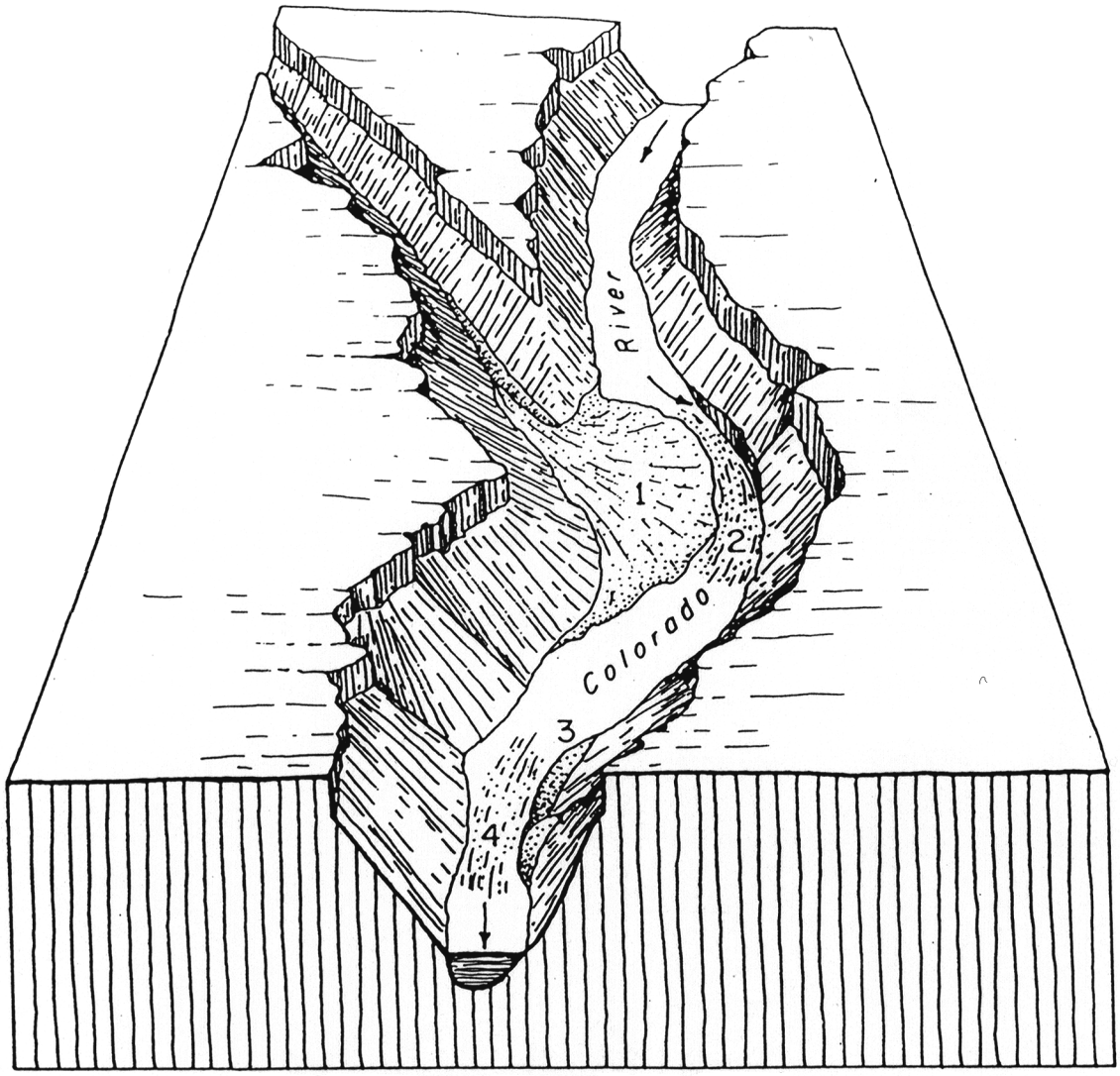

(Modified from Hamblin and Rigby, 1968)

Explanation

1. Tributary debris fan
2. Rapid controlled by large immobile boulders
3. Debris bar (synonymous with “island” or “rock garden”)
4. Riffle or rapid caused by debris bar

Figure 2. The morphology of a typical debris fan and rapid on the Colorado River in Grand Canyon.

Colorado River; metric units are used for all other measures. Use of river mile has considerable historical precedent (Stevens, 1990) and provides a reproducible method of describing the location of tributaries with respect to the Colorado River. The location of tributaries was described using river miles downstream from Lees Ferry and a descriptor of "L" for river-left and "R" for river-right. The left and right sides of the Colorado River are determined as one faces downstream.

We typically refer to "Grand Canyon" in broad reference to both Marble and Grand Canyons. "Marble Canyon" is the canyon reach of the Colorado River between Lees Ferry and the juncture with the Little Colorado River (river miles 0 to 61.5; fig. 1); we refer to Marble Canyon only for specific tributaries in that reach. Grand Canyon, which is formally designated between the juncture with the Little Colorado River and the Grand Wash Cliffs (river miles 61.5 to about 280), is considerably larger and better known than Marble Canyon. For geological and statistical reasons described in the text, we divide Grand Canyon into eastern Grand Canyon, between Lees Ferry and Crystal Rapid (river miles 0 to 98) and western Grand Canyon, between Crystal Rapid and Surprise Canyon (river miles 98 to 248; fig. 1).

Acknowledgments

The authors thank the many individuals who helped with the field and office work that made this report possible. We especially thank Dave Wegner of the Glen Canyon Environmental Studies Program, Bureau of Reclamation, for his support of our project. The professionalism of the numerous guides who piloted boats for us on the Colorado River made field work efficient, safe, and fun. Thanks also to all the people who helped with the large amount of repeat photography this study required, particularly Jim Hasbargen. Dominic Oldershaw, Dave Ring, and Sara Light-Waller performed much of the darkroom work. Chuck Sternberg drafted the illustrations. Ed Holroyd, U.S. Bureau of Reclamation in Denver, Colorado, gave extensive technical help and advice with the GIS software. Steve Sutley, of the U.S. Geological Survey in Denver, Colorado, performed all x-ray diffraction analysis. Betsy Pierson, U.S. Geological Survey, provided invaluable statistical support. We also thank Vic Baker, Jim Bennett, Yehouda Enzel, Dick Iverson, Connie McCabe, Waite Osterkamp, Tom Pierson, Steve Reneau, and Kevin Scott for their review of research design and field work in April 1991. Special thanks to Vic Baker and Jay Quade, University of Arizona, for their guidance and critical appraisal, and to Vicky Meretsky and Lauren Hammack for their critical reviews of the manuscript.

SETTING

Grand Canyon has formed where the Colorado River cuts deeply through the southwestern corner of the Colorado Plateau in northern Arizona (fig. 1), exposing nearly 2 km of Paleozoic and Proterozoic stratigraphy (fig. 3). The combination of the slow downcutting of the Colorado and the gradual rise of strata toward the Kaibab uplift in the west results in the rapid exposure of Paleozoic strata as one moves downstream (Huntoon and others, 1986). Numerous resistant strata — the Paleozoic Kaibab Formation, Coconino Sandstone, and especially the thick Redwall and Muav limestones — are exposed at river level, resulting in a narrow, steep-sided canyon. Owing to the steepness of the canyon walls, the divides for most drainages in Marble Canyon are at the rim, exposing the maximum extent of the stratigraphy. Marble Canyon encompasses much of eastern Grand Canyon.

The entire Paleozoic section and some Proterozoic units are exposed west of Phantom Ranch (river mile 87; fig. 1). The exposure of the Bright Angel Shale near river level results in a distinctly wider canyon. The drainage divides of many smaller tributaries are not at the rim; therefore, these tributaries do not contain some of the younger geologic units. The maximum dip in the regional structure is mostly to the southwest (Huntoon and others, 1986). From eastern to western Grand Canyon, increased faulting results in large changes in the elevation of stratigraphic units from one rim to the other (Huntoon and others, 1986). Western Grand Canyon lies entirely within Grand Canyon proper.

Elevations in Grand Canyon range from 975 to 2,804 m above sea level at the rim, and from 939 m to 402 m along the river. The river itself drops an

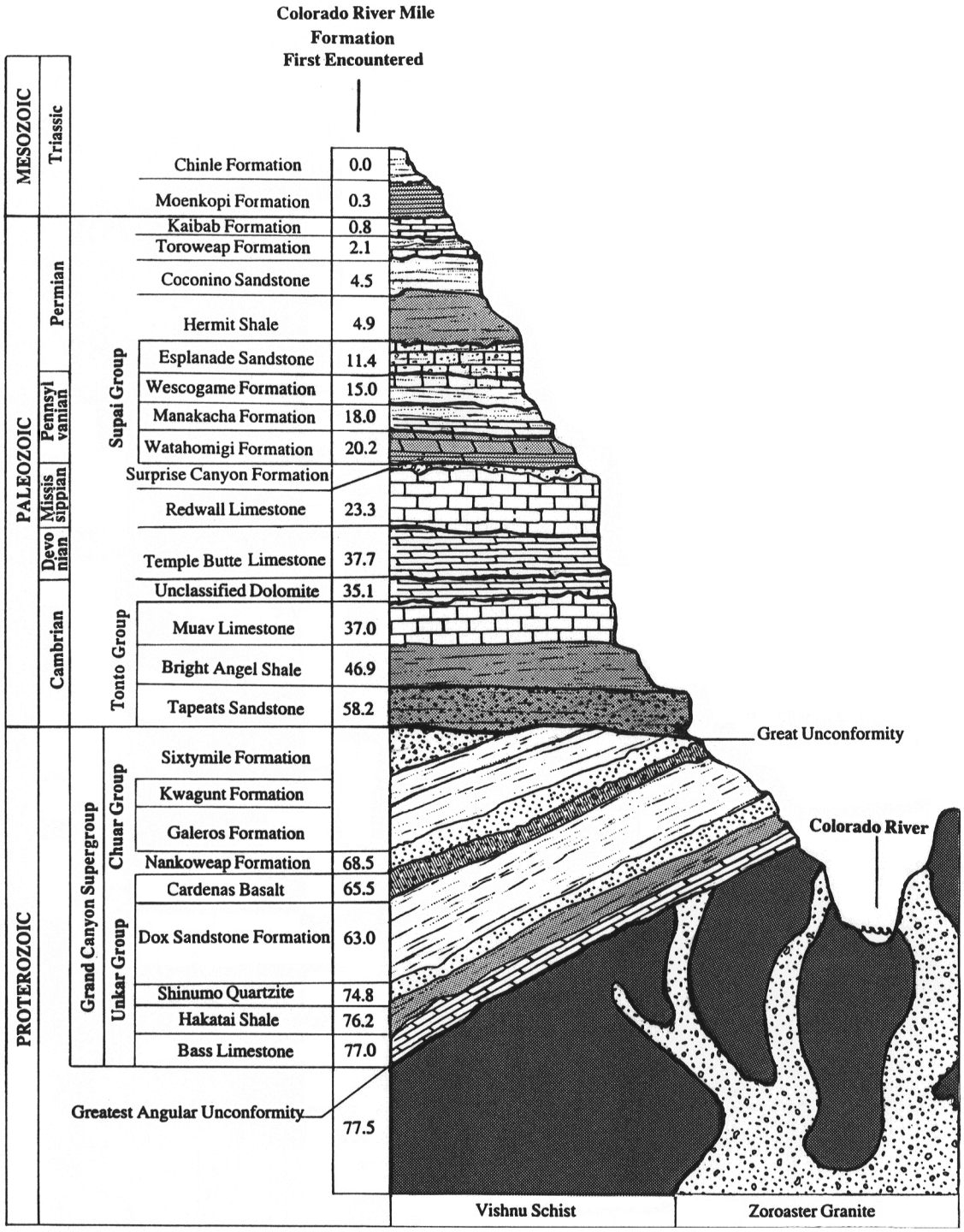

Figure 3. Stratigraphic column showing rocks exposed in Grand Canyon and the distances in river miles downstream from Lees Ferry where they first appear along the Colorado River (from Billingsley and Elston, 1989).

Table 1. Characteristics of climate stations in the vicinity of Grand Canyon National Park

Station Name[1]	Elevation (m)	Record Length	Mean Annual Precipitation (mm)	Summer Precipitation (%)	Winter Precipitation (%)
Bright Angel RS	2,726	7/48-3/95	646	29	60
Desert View	2,271	9/60-7/95[2]	347	40	48
Grand Canyon	2,204	10/04-3/95	403	42	46
Lees Ferry	978	4/16-3/95	148	50	38
Mount Trumbull	1,818	10/20-12/78[3]	297	49	37
Peach Springs	1,613	7/48-3/95	280	45	43
Phantom Ranch	834	8/66-3/95	234	39	49
Tuweep RS	1,551	7/48-12/86[4]	306	42	43

Notes:
1 All stations are in Arizona (Fig. 1).
2 Daily data from September 1, 1960, to July 1, 1975, have been lost at this station, which is not part of the NOAA network of climate stations. Monthly data is available after September 1960 from the National Park Service.
3 Station discontinued.
4 In 1986, Tuweep Ranger Station was discontinued as a cooperative observer station, which records rainfall in 0.01 in. accuracy and reports in increments of daily rainfall. A tipping-bucket recording rain gage, which records rainfall in 0.10 in. increments and reports hourly as well as daily rainfall (e.g., U.S. Department of Commerce, 1966), remains in operation.

average of 1.5 m in every linear kilometer. The climate is semiarid to arid, producing a wide range of annual and seasonal precipitation (table 1). Melis and others (1994) and Webb and others (1996) discuss the regional hydroclimatology in relation to debris-flow initiation. Precipitation generally increases with elevation, and the amount of summer precipitation generally decreases towards the west.

METHODS

Initiation Mechanisms and Precipitation Recurrence Intervals

During the course of this study (1986-1995), 25 debris flows occurred in Grand Canyon (Melis and Webb, 1993; Melis and others, 1994; Webb and Melis, 1995; Webb and others, unpublished data). For as many of these events as feasible, we traced the debris flow to its initiation point to evaluate the failure mechanism and source material. Using other reports (for example, Cooley and others, 1977), we augmented our data with data on other notable, historic debris flows.

We obtained climatic data from the National Climatic Data Center in Asheville, North Carolina, and from their reports (for example, NOAA, 1996). We used daily rainfall data, and we calculated storm precipitation by summing over consecutive days with rainfall preceding historical debris flows. We estimated the probability of daily and storm precipitation using the modified Gringorten plotting position (U.S. Water Resources Council, 1981),

$$p = ((m - 0.44)/(n + 0.12)) \bullet d, \qquad (1)$$

where p = probability of the event, m = the ranking of the event, n = the number of days in the record, and d = the number of days in the season per year. The recurrence interval, R (yrs), is

$$R = 1/p. \qquad (2)$$

Selection of Geomorphically Significant Tributaries

Melis and others (1994) identified 529 geomorphically significant tributaries to the Colorado River in Grand Canyon from Lees Ferry to Diamond Creek, excluding the four largest tributaries (the Paria and Little Colorado Rivers, and Kanab and Havasu Creeks). They selected tributaries that have the potential to produce debris flows that affect the geomorphology of the river channel. Their criteria include: 1) drainage areas larger than 0.01 km^2; 2) mapped perennial or ephemeral streams; 3) previously designated

Figure 4. Replicate photographs of the debris fan at South Canyon (river mile 32.5-R). A. Photograph taken in July 17, 1889 by Franklin A. Nims. The debris fan is relatively small, and boats were parked relatively close to the mouth of the canyon.

official name; 4) clear termination at the Colorado River in a single channel; 5) formation of obvious debris fans and (or) rapids. We extend these definitions to 71 additional tributaries between Diamond Creek and Surprise Canyon in western Grand Canyon (river miles 225 to 248).

Repeat Photography and Binomial Frequency of Debris Flows

Although there are a variety of possible methods for dating recent debris flows, including the ^{3}He, ^{14}C, and ^{137}Cs techniques (Hereford and others, 1996; Melis and Webb, 1993; Melis and others, 1994; Webb and others, 1996), the most useful method in Grand Canyon is repeat photography for historic events (Webb, 1996). Repeat photography has been used to identify changes in plant distributions, effects of operations of Glen Canyon Dam on sand bars, and the appearance of debris-flow and flood deposits in previous studies in Grand Canyon (Turner and Karpiscak, 1980; Stephens and Shoemaker, 1987; Webb and others, 1988, 1989; Melis and others, 1994; Schmidt and others, 1996; Webb, 1996). This success is in large part due to the numerous photographs that have been taken of Grand Canyon since 1872.

More than 1,039 historical photographs of the river corridor taken since 1872 have been replicated and interpreted (Melis and others, 1994). Of these, 478 photographs capture views of tributary junctures, debris fans, and rapids. By comparing photographs of a given debris fan taken at different times, we have identified geomorphic changes that indicate the occurrence of one or more debris flows during the time interval separating the photographs.

B. Replicate view taken on January 2, 1992 by Jim Hasbargen. Several debris flows have aggraded the debris fan, including a large one that deposited the prominent levee at right between 1940 and 1965.

Figure 4. Continued.

Geomorphic change in Grand Canyon is largely catastrophic in nature, especially on a decadal time scale, and changes to debris fans resulting from debris flows are usually obvious. Such changes include the appearance of new boulders and disappearance of old ones, extensions of debris fans, new debris levees, and/or large channels cut through old deposits (fig. 4). Where no debris flows have occurred, fans show few changes, even after a hundred years (fig. 5). For some tributaries, we can determine the dates of debris flows to within one year, but it is impossible to determine whether fan alteration is the result of single or multiple events. Therefore, we chose to measure binomial rather than absolute frequency for each debris fan. Instead of tallying the total number of recent debris flows at each site, we indicate simply whether or not any debris flows have occurred since 1890.

The century over which we measure the binomial frequency of debris flows is determined by a remarkable baseline of photographs taken in 1889 and 1890 by Franklin A. Nims and Robert B. Stanton (Melis and others, 1994; Webb, 1996). A total of 445 photographs record the general topography of the river corridor at roughly 2-km intervals along the entire length of Grand Canyon. We replicated the Nims and Stanton photographs between 1990 and 1994 (Webb, 1996); in addition, we used 38 photographs of the Canyon taken by John K. Hillers in 1872 (Fowler, 1989). A total of 178 of these 483 photographs capture debris fans at the confluences of 164 of the 600 tributaries and the

Figure 5. Replicate photographs showing the debris fan at Ruby Rapid (river mile 104.8-L) (Webb, 1996). A. Photograph taken on February 15, 1890 at 1:00 PM by Robert B. Stanton. Lack of sand in the canyon mouth, and fresh-looking gravels all the way to the river, indicates a flash flood had recently occurred in Ruby Canyon, probably in the summer of 1889.

Colorado River in Grand Canyon (fig. 6). These 164 fans form the "calibration set" of our data.

One important limitation of this data set is that the photographic record captures only the mouths of the tributary canyons. Thus, binomial-frequency estimates are skewed to record only those debris flows large enough to reach the Colorado River. Therefore, we do not include all debris flows generated in tributaries, but only those that have reached the river.

Morphometric, Lithologic, and Climatic Variables

We measured 21 variables representing the morphometric, lithologic, climatic and structural drainage-basin characteristics that may control or influence debris-flow initiation in Grand Canyon (table 2). These include standard drainage-basin measures such as area, channel length, and channel gradient. All three major debris-flow source lithologies (Hermit Shale, the Supai Group, and Muav Limestone) are represented by their height above river level, a measure of the potential energy of source failures. We also included the height above river level of the highest point in each drainage basin. Although this variable does not relate directly to source failures, it does reflect the potential for intense rainfall and the potential energy of runoff, which are factors in some types of failures. A large amount of initial energy may not translate into a debris flow, however, if the transit distance to the river is sufficiently long. The greater the distance, the more energy is lost in transit (Savage and Hutter, 1987), and fewer and smaller debris flows reach the river. Therefore, we also measured channel distance from each source lithology to the river. The inter-dependence of source height and channel distance from river are represented in a third class of variable, channel

B. Replicate view taken on February 14, 1991 at 2:11 PM by T.S. Melis. Despite higher water in 1991, the rapid and debris fan are unchanged after a century. Erosion and deposition by the Colorado River have caused the only changes in the debris fan. Instead of fresh-looking gravels at the mouth of the canyon, cobbles and boulders are now exposed. A large sand bar has been deposited at right center, obscuring a clear view of the channel mouth.

Figure 5. Continued.

gradient from source area to river, a simple ratio of channel distance to source height.

Few Grand Canyon tributaries have climatic stations, so precipitation associated with debris flows must be estimated using data collected many kilometers away. Because of this, we derived proxy variables to measure climatic effects on debris-flow initiation. Elevations of source lithologies and basin headwaters above sea level are included to reflect orographic effects on precipitation. Higher elevations are likely to intercept more moisture as precipitation and so produce more debris flows. Additionally, tributaries which open into the dominant paths of weather systems and moisture vectors may actively trap precipitation, particularly smaller storms. Tributaries facing other directions may be orographically shielded from many storms.

We calculated the aspect, F, for each drainage as the angle from true north of a ray drawn from the basin centroid to its confluence with the river. This radial measure was then transformed into a linear value more appropriate for logistic regression modeling: southwestern aspect (θ), the degree to which a given drainage faces southwest using

$$\theta = \sin[(\Phi - 45°)/2]. \quad (3)$$

An orientation to the southwest was chosen to reflect the southwest to northeast travel vectors of severe weather across Grand Canyon. Similarly, we measured the aspect of the canyon or river-corridor itself as the angle from true north of a vector drawn parallel to the river at the confluence of each tributary. This value, which we termed Θ, was linearized into a variable of southwest/northeast trend in the river corridor runs using

Table 2. Drainage-basin parameters used in logistic regression

Variable	Variable name	Approximate[1] probability distribution	Range in values	Units
Drainage-basin area	AREA	lognormal	-1.3 to 3.8	km^2
Height above river of:				
- headwaters	HEADHT	normal	402 to 2207	m
- Hermit Shale	HERMHT	bimodal normal	0 to 1488	m
- Supai Group	SUPHT	bimodal normal	0 to 1134	m
- Muav Limestone	MUHT	bimodal normal	0 to 890	m
Inverse of channel length to:				
- headwaters	HEADD	lognormal	-1.8 to 0.3	$\log (m)^{-1}$
- Hermit Shale	HERMD	bimodal lognormal	-3.0 to 0.7	$\log (m)^{-1}$
- Supai Group	SUPD	bimodal lognormal	-3.0 to 1.0	$\log (m)^{-1}$
- Muav Limestone	MUD	bimodal lognormal	-3.0 to 1.0	$\log (m)^{-1}$
Channel gradient to:				
- headwaters	HEADG	lognormal	-1.8 to 0.3	none
- Hermit Shale	HERMG	bimodal lognormal	-3.0 to 0.7	none
- Supai Group	SUPG	bimodal lognormal	-3.0 to 0	none
- Muav Limestone	MUG	bimodal lognormal	-3.0 to -0.2	none
Elevation of:				
- headwaters	HEADEL	normal	1061 to 2804	m
- Hermit Shale	HERMEL	bimodal normal	0 to 2073	m
- Supai Group	SUPEL	bimodal normal	0 to 1951	m
- Muav Limestone	MUEL	bimodal normal	0 to 1707	m
Tributary aspect	TASP	uniform	0 to 1.0	none
River aspect	RASP	uniform	0 to 1.0	none
Log of total length of faults	FAULT	normal	-2 to 2.3	log (km)
River kilometer	RKM	uniform	4.5 to 395.9	km

[1] Bimodal normal, the distribution is normal except for zero values. Bimodal lognormal, the distribution is lognormal except for transformed zero values.

$$\Theta = |\cos(\Phi - 45°)|. \quad (4)$$

The influence of geologic structure in each drainage was evaluated as the linear sum of all surface faults delineated on geologic maps of the area (Haynes and Hackman, 1978; Huntoon and others, 1981; Huntoon and Billingsley, 1983; Huntoon and others, 1986). One important difficulty with these data is that geologic map coverage of the study area is not at a uniform scale: map scales ranged from 1:250,000 to 1:48,000. Thus, on the basis of scale variation alone, apparent fault density may differ from one area to another depending on the map used. In this case, fault density may increase artificially from east to west, because map scales increased in that direction.

We also included a measure of river kilometer, the distance in kilometers along the river from Lees Ferry to the confluence with each tributary. This variable is intended to reflect any ordered spatial variation in debris-flow frequency along the river corridor that is not accounted for by the other variables.

All drainage-basin data were measured from USGS 7.5' topographic maps (1:24,000 scale) and various geologic maps (Haynes and Hackman, 1978; Huntoon and others, 1981; Huntoon and Billingsley, 1983; Huntoon and others, 1986). For source lithologies, elevations, heights above and channel distance from the river, we averaged the largest and smallest values measured to the bottom

of the units. We calculated an inverse-channel distance variable, which is the reciprocal of channel distance. For lithologic strata that are not present in a given basin, zero values were entered for their variables. Gradient was calculated simply as height above river divided by channel distance, and so is also a mean value. Drainage-basin boundaries were drawn by hand on topographic maps, digitized, and entered into a GIS, which calculated drainage areas and centroids.

Statistical Procedures

Because the dependent variable, debris-flow frequency, is binomial, we chose logistic regression for modeling the relation of drainage-basin variables to debris-flow frequency. Where linear regression returns a continuous value for the dependent variable, logistic regression returns the probability of a positive binomial outcome (in this case, debris-flow occurrence during the last century). Logistic regression is commonly used in medical and biological studies where the dependent variable is the presence or absence of a given illness or disease, and independent variables the presumed controlling factors. In medical research, logistic regression is used to analyze the statistical significance of certain factors in relation to diseases, as well as for modeling the probability of contracting the disease on the basis of the significant controlling factors (Hosmer and Lemeshow, 1989).

For logistic regression, the conditional mean probability, ($\pi(\mathbf{x})$) is:

$$\pi(x) = e^{g(\mathbf{x})} / [1 + e^{g(\mathbf{x})}], \qquad (5)$$

where

$$g(\mathbf{x}) = \beta_0 + \beta_1 x_1 + \beta_2 x_2 + ... + \beta_i x_i \qquad (6)$$

and i = number of variables. The coefficients (β_v) are estimated by the method of maximum likelihood, where coefficients with the highest probability of returning the observed values are selected. Maximum likelihood is determined using the likelihood function, which expresses the probability of the observed data as a function of the unknown coefficients (Hosmer and Lemeshow, 1989). Those coefficients that maximize the likelihood function are thus the coefficients with the greatest probability of returning the observed values. SAS statistical software was used to calculate these model coefficients as well as various measures of their significance (SAS, 1990). After the coefficients are estimated using the calibration set, and verified as reasonable using the verification set, we calculated the probabilities of debris-flow occurrence for all 600 tributaries using equations (5) and (6).

Our 9,516 km^2 study area is too geomorphically diverse to be effectively treated in one model of Grand Canyon; drainage-basin lithology and morphology differ markedly over the length of the Colorado River. Instead, we separated the initial 164 drainages with known debris-flow frequencies into two distinct data sets, one each for eastern and western Grand Canyon. It is extremely difficult to identify a unique point of geomorphic transition between the eastern and western canyon as a variety of major structural and morphometric changes occur between Phantom Ranch (river mile 97.8) and Crystal Creek (river mile 98.2). The margin faults passing across Grand Canyon at Crystal Creek (Hunter and others, 1986) suggested that mile 98 was the approximate point of separation between eastern and western Grand Canyon. Splitting the data at river mile 98.0 (Crystal Creek) resulted in models that presented the best balance in terms of model fit and stability. Moving the point of separation east or west from this location excessively strengthened one model at the expense of the other. Separating the data at river mile 98.0 placed 78 drainages in eastern Grand Canyon (river mile 0 to 98.0) and 86 drainages in western Grand Canyon (river mile 98.1 to 248.3). These data, which we call the "calibration set," do not represent a random sample of our population, based as they are on the historical photographic evidence available to us. Nevertheless, a comparison of the sample and population distributions of each drainage-basin variable indicates that the sample is statistically representative of the population of ungaged tributaries throughout Grand Canyon (fig. 6).

We used principal-component analysis to identify the drainage-basin variables that are statistically redundant. After a qualitative assessment of the redundant variables that contribute to the effectiveness of the model (usually

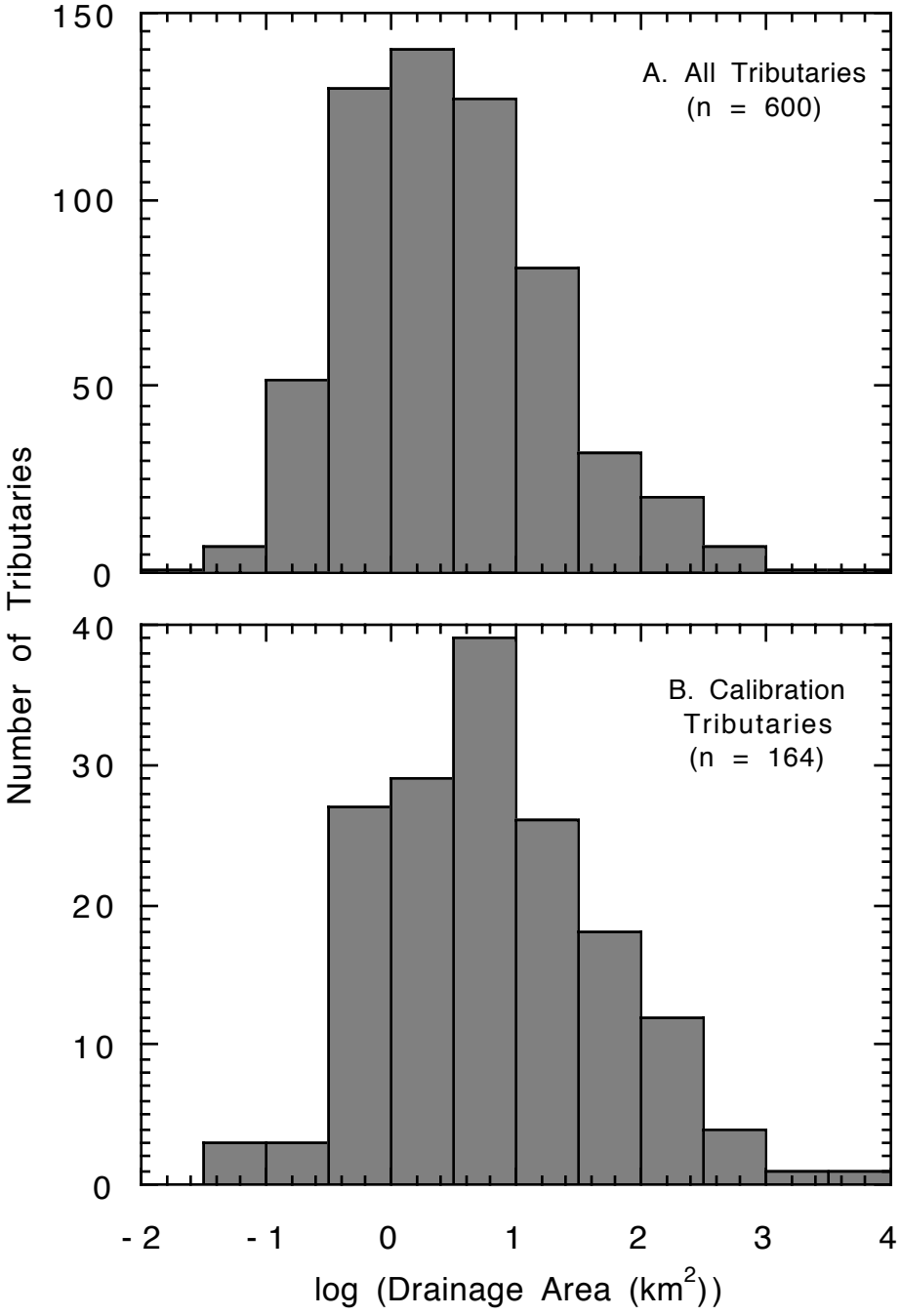

Figure 6. Histograms comparing the sample drainage-basin areas with the population drainage-basin areas of tributaries in Grand Canyon.

on the basis of increased information content), the extraneous variables were eliminated from further consideration. Variables measuring distance or area, such as drainage area, channel distances, channel gradient, and fault distance, are distributed logarithmically. Logistic regression is not dependent on normally distributed data, but log transformation of these variables reduces the redundancy identified by principal-component analysis. We therefore chose to use the log-transformed values in modeling the probability of debris-flow occurrence. To properly evaluate zero values in log-transformed data, zero values were replaced with a value one order of magnitude smaller than the smallest non-zero variable. For source-lithology channel distances and gradients this value was 0.001, resulting in a log-transformed value of -3. For fault lengths, these values were 0.01 and -2.

We used a step-backward elimination process in our logistic regression (SAS, 1990). Variables of least statistical significance are removed from the model until only variables with significance (ρ_v) less than a given threshold (0.10 in this study) remain. We used the χ^2 measure of the Wald statistic (Hosmer and Lemeshow, 1989; SAS, 1990) to evaluate variable significance. We employed several statistics to evaluate the quality of the resulting models. These statistics include measures of the overall significance of the final model compared with the model containing all initial variables (ρ_m); a percentage of accurately predicted debris-flow occurrence as a rough measure of model accuracy (α); and the Hosmer/Lemeshow model goodness-of-fit statistic (C), which can be expressed as a χ^2 significance measure (ρ_C) (Hosmer and Lemeshow, 1989).

We also calculated the odds ratio (Ψ) for each variable in the model. This statistic measures the change in the odds of outcome occurrence per unit increase of the variable. We evaluated how robust the models were by attempting to reproduce model results using larger data sets drawn from the same population of drainages. For this purpose, we determined debris-flow probability for the "verification set," an additional 50 drainages — 25 each in eastern and western Grand Canyon — using a variety of non-photographic methods, including radiometric dating, stratigraphic evidence, and other field evidence (Melis and others, 1994). Unfortunately, a verification set of only 25 observations is too small for reliable logistic regression modeling alone. We therefore added each set of 25 drainages to the original calibration data and formed two larger verification data sets (fig. 7). This overlap of calibration and verification data limits the usefulness of the model comparison.

INITIATION OF DEBRIS FLOWS

Debris flows in Grand Canyon are initiated by a combination of intense precipitation and subsequent slope failure. The intensity of rainfall necessary to initiate debris flows in Grand Canyon is poorly known because few climatic stations are in debris-flow producing tributaries. Previous studies have reported rainfall that initiates debris flows to have intensities greater than 25 mm/hr with a total rainfall of at least 16 to 50 mm (Webb and others, 1989; Melis and others, 1994). The recurrence interval of precipitation on the days when debris flows have occurred in Grand Canyon ranges from less than one year to more than sixty years (table 2). Multiday storms that precede debris flows had larger recurrence intervals, typically greater than 100 years.

Intense precipitation may occur in summer or winter throughout Grand Canyon. Three types of storms can cause floods in the southwestern United States: localized or widespread convective thunderstorms in summer, regional frontal systems in winter, and dissipating tropical cyclones in late summer and early fall (Hansen and Shwarz, 1981; Hirschboeck, 1985; Webb and Betancourt, 1992; Thomas and others, 1994). Most historic debris flows in Grand Canyon are associated with the intense precipitation of convective summer thunderstorms that affect only one or two drainages at a time. These storms are fed by large quantities of moisture, evaporated from the northern Pacific and Gulf of California by monsoonal circulation patterns. Debris flows also occur during prolonged precipitation produced in winter by regional frontal systems (Cooley and others, 1977). These widespread storms sweep across the Colorado Plateau from the west along the Pacific storm track, which is shifted south during the winter by the Aleutian Low in the North Pacific Ocean (Webb and Betancourt, 1992). Rain that can be both

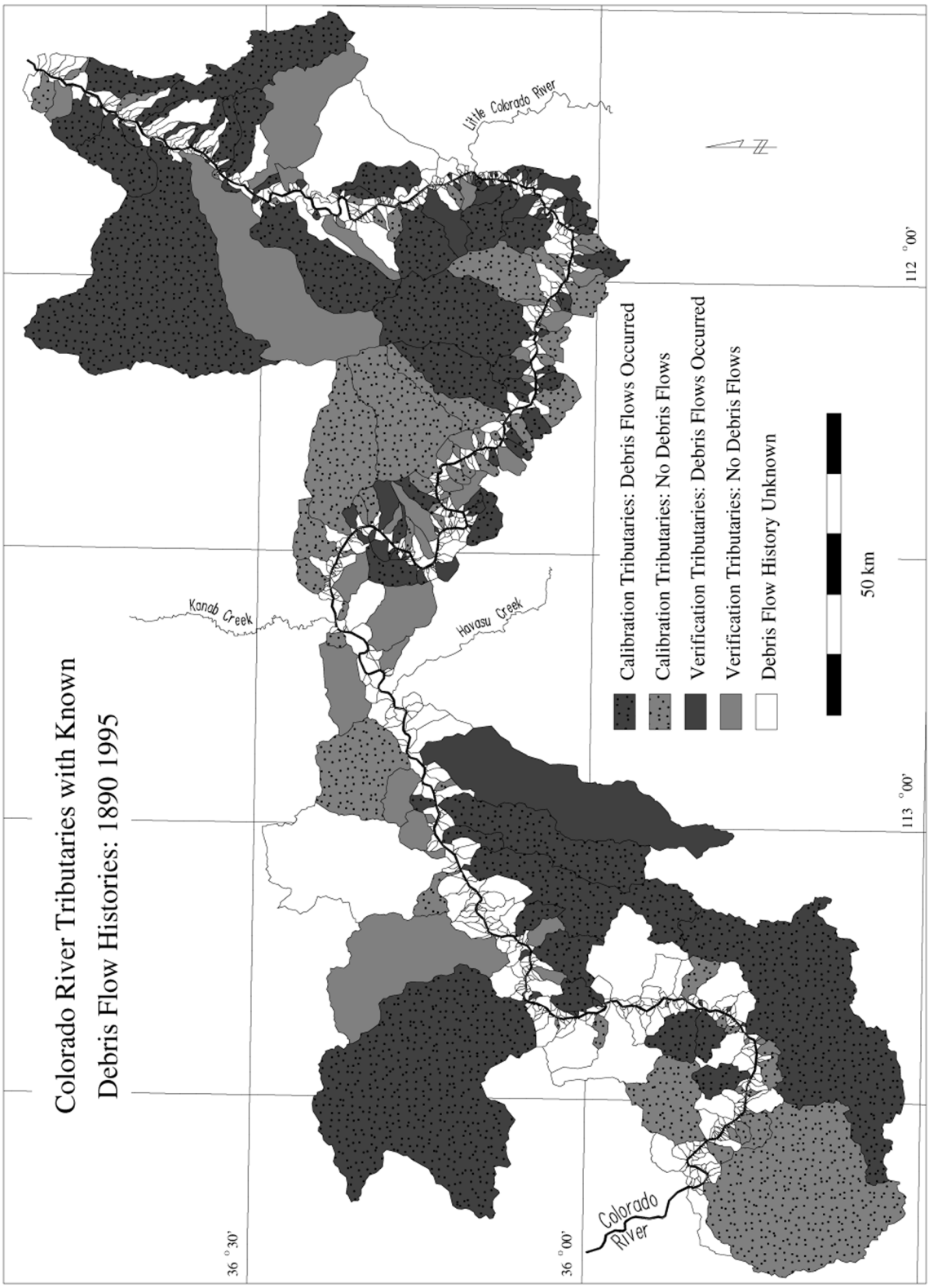

Figure 7. Map of Grand Canyon showing the locations of tributaries with histories of debris flows between 1890 and 1990.

Table 3. Precipitation associated with selected debris flows in Grand Canyon

Tributary	River mile -side	Basin area (km^2)	Date of debris flow	Nearest climate station	Daily precip-itation (mm)	Recurr-ence interval (years)	Storm[1] precip-itation (mm)	Recurr-ence interval (years)
Badger Canyon	7.9-R	47.0	8/18/94	Lees Ferry	45	46	45	16
18-Mile Wash	18.0-L	5.1	8/24/87	Desert View	14	<1	17	<1
Unnamed	19.9-L	3.8	8/24/87	Desert View	14	<1	17	<1
Unnamed	62.5-R	0.7	9/18/90	Desert View	19	<1	61	34
Crash Canyon	62.6-R	1.8	9/18/90	Desert View	19	<1	61	34
Unnamed	63.4-R	0.7	9/18/90	Desert View	19	<1	61	34
Lava Canyon	65.5-L	54.7	12/5/66	Grand Canyon	43	16	118	157
Tanner Canyon	68.5-L	19.3	8/22/93	Desert View	28	3	56	8
Cardenas Creek	70.9-L	3.9	8/22/93	Desert View	28	3	56	8
Unnamed	71.2-R	1.1	8/21/84	Grand Canyon	35	3.2	69	7.6
Unnamed	72.1-R	1.2	8/21/84	Grand Canyon	35	3.2	69	7.6
75-Mile Creek	75.5-L	11.5	8/24/87	Desert View	14	<1	16	<1
			9/18/90	Desert View	19	<1	61	34
Monument Creek	93.5-L	9.7	7/27/84	Grand Canyon	27	1	39	1
Hermit Creek	95.0-L	32.0	7/15/96	Grand Canyon				
Crystal Creek	98.2R	111.6	12/6/66	Tuweep	96	63	157	63
Forster Canyon	122.7-L	10.0	9/8/91	Grand Canyon	13	<1	18	1.9
Fossil Canyon	125.0-L	34.4	8/19/89	Grand Canyon	46	8	92	25
Unnamed	126.9-L	0.6	8/19/89	Grand Canyon	46	8	92	25
Unnamed	127.3-L	0.8	8/19/89	Grand Canyon	46	8	92	25
Unnamed	127.6-L	1.8	8/19/89	Grand Canyon	46	8	92	25
Bedrock Canyon	130.5-R	21.1	8/19/89	Grand Canyon	46	8	92	25
Unnamed	157.6-R	11.1	8/6/93	Peach Springs	20	<1	22	<1
Unnamed	160.8-R	3.4	8/6/93	Peach Springs	20	<1	22	<1
Prospect Canyon	179.4-L	257.2	9/6/39	Grand Canyon	32	7	98	158
			7/24/54	Grand Canyon	27	1	27	--[2]
			7/24/55	Mount Trumbull	111	100	112	100
			9/17/63	Mount Trumbull	23	<1	23	<1
			3/5/95	Tuweep	43	5	--[2]	--[2]
Unnamed	207.8-L	3.1	9/23/91	Peach Springs	35	3	--[2]	--[2]
Diamond Creek	225.8-L	716.7	7/20/84	Tuweep	53	10	90	24

[1] Storm is defined as consecutive days with measurable rainfall.
[2] One day storm.

widespread and intense is produced by occasional dissipating tropical cyclones in the late summer and early fall (Smith, 1986), but these storms have only caused debris flows in Prospect Canyon (Melis and others, 1994; Webb and others, 1996).

In general, moisture and storm systems travel across Grand Canyon from west to east and south to north. Strong orographic lifting occurs in the vicinity of the Kaibab Plateau, with greater rainfall falling at higher elevations (table 1). It should be noted that, although intense or prolonged rainfall is necessary for the occurrence of a debris flow, rainfall alone is not a sufficient cause because a slope failure is also required (Melis and others, 1994). The occurrence of debris flows cannot be predicted solely on the basis of rainfall.

Figure 8. Debris-flow source areas exposed in Monument Creek (river mile 93.5-L), Grand Canyon, Arizona. The Supai Group forms the dark, ledgy unit in the middle of the section; the overlying slope is Hermit Shale. The 1984 debris flow was initiated in the Hermit Shale and the lowest member of the Supai Group (Webb and others, 1988).

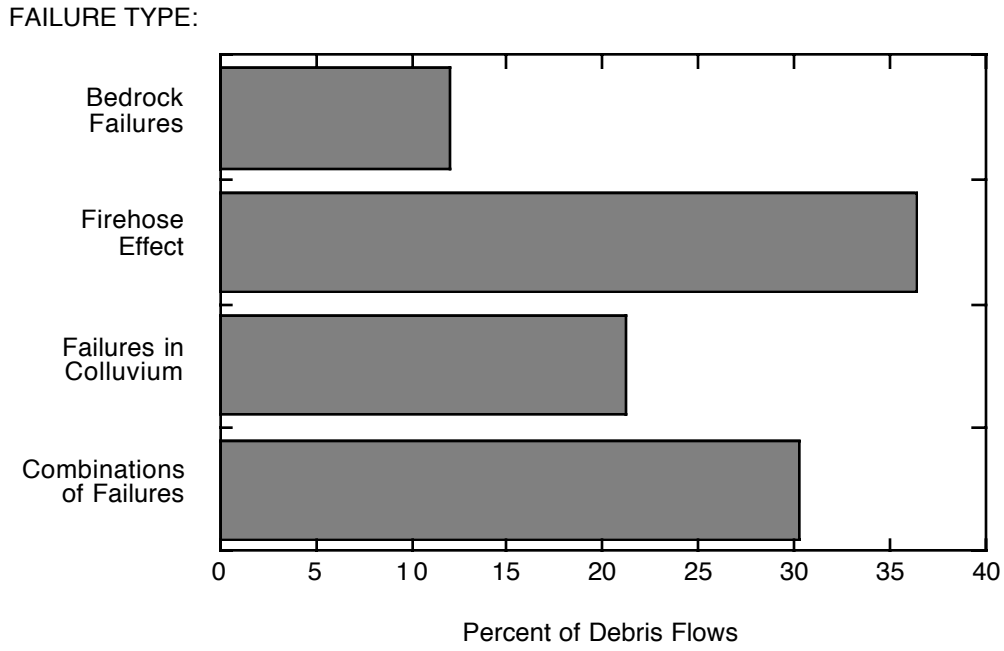

Figure 9. Failure mechanisms that have initiated debris flows in Grand Canyon from 1939 through 1996 (modified from Melis and others, 1994).

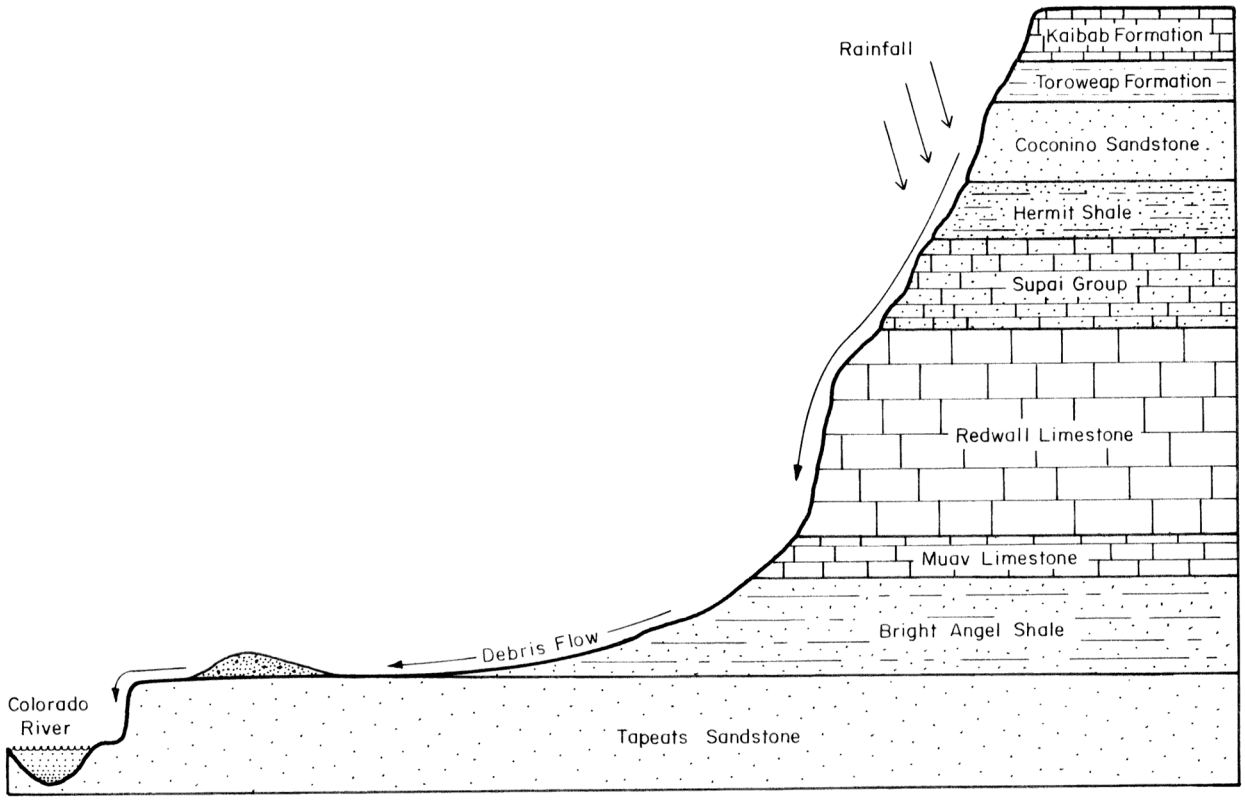

Figure 10. Schematic diagram illustrating the initiation of debris flows by the failure of bedrock - usually the Hermit Shale and Supai Group - during intense rainfall.

Debris-flow source sediments in Grand Canyon consist of weathered and jointed bedrock, colluvial wedges, or sediment stored in or adjacent to channels. Numerous exposed Paleozoic and Proterozoic strata, ranging from shale to sandstones and limestones, provide many types of source rock in a setting of high topographic relief (figs. 3, 8). Weathering and erosion are constantly at work on these strata as the canyon continues to widen (Ford and others, 1974; Webb and others, 1989; Hereford and Huntoon, 1990; Melis and others, 1994). Elevational and temperature gradients, along with a high degree of annual and inter-annual climatic variability, promote rock expansion/contraction as well as precipitation-related infiltration and frost action. All Grand Canyon drainage basins, particularly the largest ones, are influenced to some extent by regional and localized faults, folds and joints, which weaken bedrock to various degrees. Soft shale units erode quickly, and can destabilize overlying cliffs of more indurated sandstones and limestones. These processes result in rockfalls and rock avalanches that occur in all seasons, and under a wide variety of weather conditions, but are especially common during the winter due to prolonged precipitation and freezing temperatures. Larger slab failures also occur in the more indurated sandstones, especially the Coconino and Esplanade Sandstones, as compressive stresses are released during erosive unloading.

Rockfalls and slab failures do not necessarily produce debris flows, but they do produce large amounts of colluvium that is an important source material for debris flows. This colluvium collects where softer units have eroded to form benches, particularly the Hermit Shale and the distinctive Tonto Platform formed by the Muav Limestone and Bright Angel Shale (figs. 1, 3). Various shale units within the members of the Supai Group form smaller, high-angle slopes that also collect loose debris (fig. 8).

Other sources of loose, poorly sorted debris are shear zones in the many fault-controlled drainages present in Grand Canyon, such as 75-Mile Canyon (river mile 75.5-L). This tributary has formed along the strike of east-trending 75-Mile Fault, and drainages have formed preferentially along the highly fractured, footwall-side of the fault. Since 1959, three debris flows have been initiated exclusively in colluvium accumulated in these footwall sub-basins (Melis and others, 1994). Alluvial deposits, especially old debris-flow levees along the sides of tributary channels, also provide source sediments. Once initiated, debris flows in Grand Canyon often "bulk up", entraining sediments from terrace deposits and gaining volume and velocity as they head toward the river (Melis and Webb, 1993; Melis and others, 1994; Webb and others, 1996).

Melis and others (1994) identified four main mechanisms of debris-flow initiation in Grand Canyon: 1) the failure of weathered bedrock; 2) the "firehose effect" of runoff falling onto unconsolidated colluvial wedges, 3) direct failure of colluvial wedges, 4) combinations of the first three mechanisms (fig. 9). We extend the data from Melis and others by adding information from debris flows that occurred between 1994 and 1996. The largest debris flows — which are few in number — begin with the failure of weathered Paleozoic shales and sandstones, most often in either the Hermit Shale or Supai Group, although failures also occur in other formations such as the Bright Angel Shale (fig. 10). Bedrock failures are most often triggered by intense, localized rainfall from convective summer thunderstorms, although bedrock failures occurred in the December 1966 debris flow (Cooley and others, 1977). One example of this failure mechanism occurred during the Monument Creek (river mile 93.5-L) debris flow of 1984 (Webb and others, 1988, 1989). On July 25, runoff from a thunderstorm centered over the eastern part of Monument Creek caused a slope failure in the Esplanade Sandstone. The failure became an avalanche that fell 650 m and mobilized into a debris flow upon reaching the creek channel. The debris flow traveled 4.5 km to the Colorado River where deposition of boulders significantly altered flow in Granite Rapid (Webb and others, 1988).

Most debris flows in Grand Canyon are produced by the "firehose effect." In this mechanism, runoff pours over a cliff face and impacts colluvium at the base of the cliff, causing bulk failure (Johnson and Rodine, 1984). This process frequently occurs in drainages that have high-elevation catchments, leading to waterfalls over the Redwall Limestone, with runoff falling on colluvium that overlies slopes of Muav Limestone and Bright Angel Shale (figs. 11, 12). As with bedrock failures, the firehose effect is usually

triggered by small summer thunderstorms but can also occur during less-intense regional storms, especially in large tributaries that concentrate runoff at a single pourover. The firehose effect triggered a debris flow in "Crash Canyon" (river mile 62.6-R) on or about September 18, 1990 (Melis and Webb, 1993). Runoff from convective thunderstorms poured over the Redwall Limestone cliffs of Chuar Butte, falling onto massive colluvial deposits overlying Muav Limestone. The colluvium failed, resulting in a debris flow (Melis and others, 1994).

Failures of colluvial wedges occur during either intense or prolonged rainfall, and usually result in smaller debris flows. In the case of low-intensity, sustained rainfall, saturation may be hastened by concentrated sheetflow runoff from cliff faces. This substantial runoff is focused at the intersection of colluvial wedge and cliff face, augmenting direct precipitation and increasing the rate of saturation. The probability of slope failure is enhanced by the low density of vegetation on talus slopes in Grand Canyon. Multiple source areas combined with the extreme topographic relief of Grand Canyon can result in combinations of the three basic initiation mechanisms.

Importance of Shale

Shales are a critical factor in the initiation of debris flows in the Colorado River drainage basin. Weathered shale bedrock fails readily, either producing debris flows directly or contributing source material to colluvial wedges. Shales form the slopes in Grand Canyon and store unconsolidated source material. If colluvial wedges do not fail, the underlying bedrock may fail, mobilizing the overlying colluvium. Eroding shales also undercut more-indurated, cliff-forming lithologies, contributing to their failure. Of most importance, shales in Grand Canyon provide abundant fine particles and clay minerals that are essential to the mobility and transport competence of debris flows, giving them the internal strength necessary to transport large boulders over long distances. Electrochemical attraction among clay particles increases debris-flow matrix strength, and strong water absorption helps maintain high pore pressures, one condition deemed necessary to support large clasts (Hampton, 1975; Pierson and Costa, 1987; Major and Pierson, 1992). Most Grand Canyon debris flow deposits contain 1-8 percent silt- and clay-size particles by weight (fig. 13); the exception is Prospect Canyon, which has a unique setting for debris-flow initiation (Webb and others, 1996). These fine particles occupy interstitial spaces in debris-flow slurries, increasing the density of the matrix and the buoyant forces that contribute to the suspension of larger particles (Beverage and Culbertson, 1964; Hampton, 1975; Rodine and Johnson, 1976). Fine-grained constituents of these debris flows are 60-80 percent illite and kaolinite by weight, reflecting the terrestrial source shales and colluvial wedges (table 4).

Three lithologic units dominate the initiation sites for debris flows in Grand Canyon. The Hermit Shale is the most important unit of the three source areas in terms of generating debris flows. This shale is prone to both bedrock and colluvial failures, and undermines the overlying Coconino Sandstone, a source of many large boulders in eastern Grand Canyon, as it erodes. Where the Hermit Shale is first elevated to heights over 100 m above the Colorado River (about river mile 20.0), a set of some of the most closely-spaced rapids in Grand Canyon, informally termed "the Roaring Twenties," begins (fig. 1). Although the lithology and structure of the canyon have not changed significantly at this point, the elevation of the Hermit shale beyond a threshold height above the river gives failures sufficient potential energy to transform into debris flows. Beyond this stretch of river, the Hermit Shale remains a key factor in debris-flow initiation, but may be too high on the cliffs to occur in the smaller drainages. In smaller tributaries without exposures of Hermit Shale, the lower units of the Supai Group or colluvial wedges of the Tonto platform become more important in generating debris flows. Terrestrial shales in the Supai Group — particularly the basal unit of the Esplanade Sandstone — are also major sources of bedrock failures, providing both fine particles and large boulders from interstratified shale and sandstone units. Many failures occur in the Esplanade Sandstone, which is undercut by erosion of the basal shale unit. The Muav Limestone contains thin, interbedded shales and grades into the underlying marine Bright Angel Shale. The

Figure 11. Failure scars caused by the “firehose effect” on colluvial wedges overlying Muav Limestone at river mile 62.5-R, Grand Canyon, Arizona (photograph is by T.S. Melis).

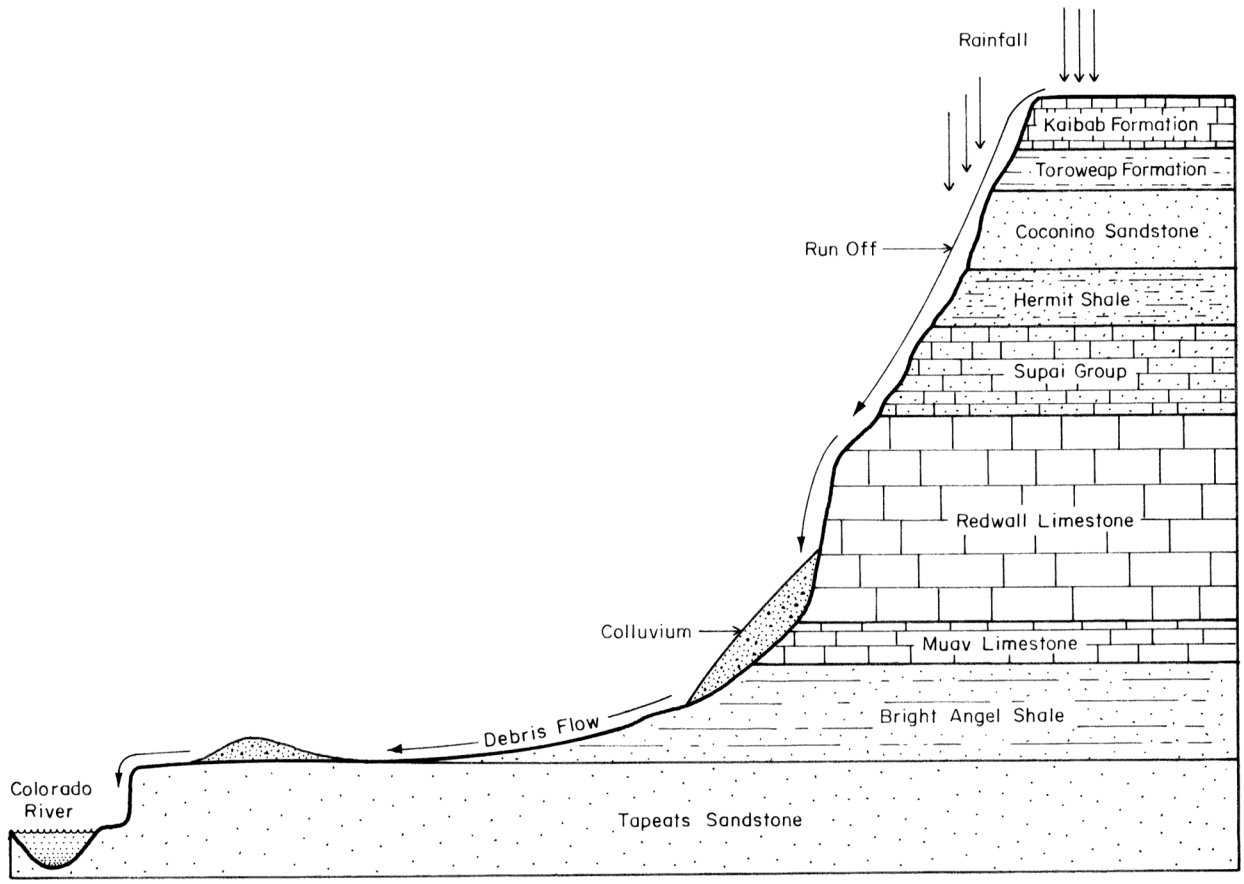

Figure 12. Schematic diagram illustrating the initiation of debris flow by colluvial wedge failure during intense rainfall.

erosional shelf formed by these units is the Tonto Platform, a broad shelf at the base of the Redwall Limestone that stores abundant colluvial material throughout Grand Canyon downstream from river mile 60 (fig. 1).

From the time of the first exploration of Grand Canyon by John Wesley Powell in 1869, the occurrence of rapids in Grand Canyon has been linked to the presence of resistant bedrock at river level (Powell, 1875). The large boulders that form rapids are well-indurated and derive from resistant bedrock units, but they have been rafted down to the river from tributary side canyons, often over many kilometers, by debris flows. The initiation of these debris flows is dependent on the presence of exposed shale units as both points of initiation and sources of fine materials. Debris flows in Grand Canyon, and ultimately the rapids they form, depend on the presence of shale source units exposed at greater than 100 m above the Colorado River. Without the combination of exposed shale units at height and boulder-producing sandstones and limestones, debris flows that form rapids will rarely occur.

LOGISTIC-REGRESSION ANALYSES

Eastern Grand Canyon

A principal-component analysis of the drainage-basin data for eastern Grand Canyon identified 9 redundant variables (fig. 14). Variables measuring height above and channel distance to the river were eliminated in favor of elevation and gradient variables, respectively. The river kilometer variable was also removed, as it strongly reflects the variation in Muav Limestone. The elevation and gradient of Muav Limestone were also strongly related, but both were retained as their removal had no effect on model outcome.

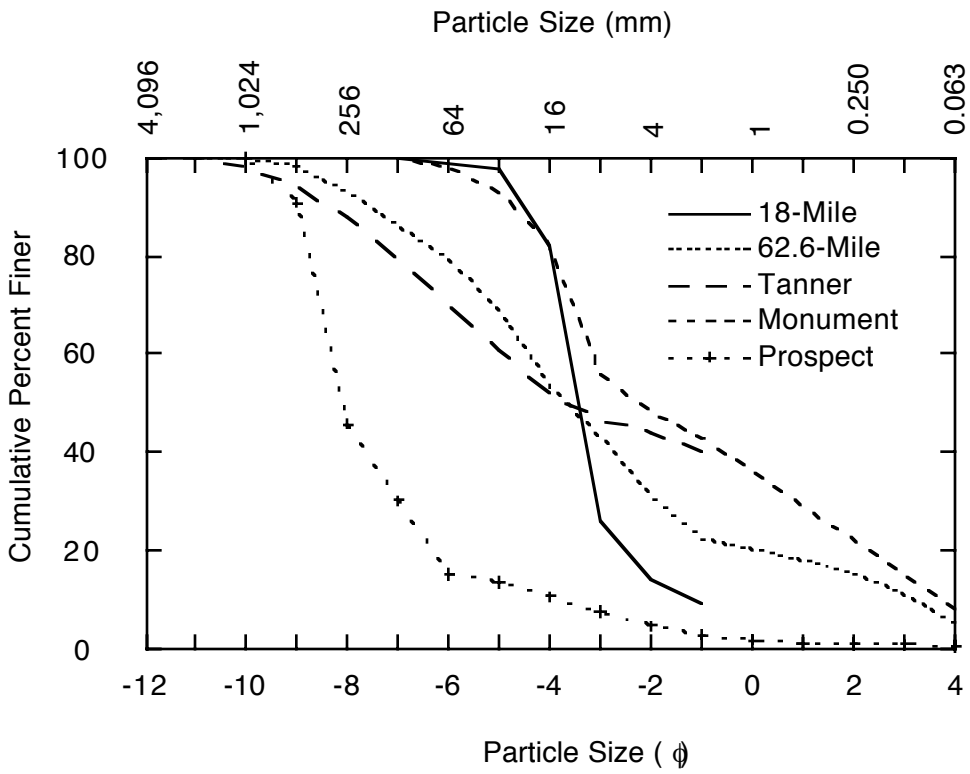

Figure 13. Particle size distribution of selected debris flows in Grand Canyon (Webb and others, 1989; Melis and others, 1994). 18-Mile, the 1987 debris flow at 18-Mile Wash; 62.6-Mile, the 1990 debris flow at "Crash Canyon," mile 62.6-R; Tanner, the 1993 debris flow at Tanner Canyon; Monument, the 1984 debris flow in Monument Creek; and Prospect, the 1995 debris flow in Prospect Canyon.

A significance threshold of 0.10 was used in modeling the binomial frequency of debris flows from the remaining 12 drainage-basin variables. Backwards, stepwise elimination removed eight variables as statistically insignificant (table 5). Overall model significance, ρ_m, is 0.86, indicating no significant difference between the final, five-variable and the original, twelve-variable model. This implies that there is a clear distinction between significant and non-significant variables. Model accuracy in predicting observed binomial frequencies is 76 percent, and $\rho_C > 0.41$, suggesting an adequate fit to the observed data. The verification set generated a model with the same group of significant variables (table 6), indicating that the calibration model is robust.

The high statistical significance of a climatic variable, river aspect ($\rho_v = 0.002$), reflects both the essential role of precipitation in debris-flow initiation and regional structure. A positive correlation with debris-flow frequency indicates that more debris flows occur where the river corridor trends northeast to southwest, directly along the path of most severe storms that track across the canyon. This correlation most likely relates to the general morphology of Grand Canyon, which is a narrow, deep canyon cut into a large plateau. Where the canyon trends southeast to northwest, perpendicular to the vector of severe weather and regional structure, storms may quickly cross the canyon and dissipate without dropping into it. This quick passage and dissipation results in less precipitation and limits intense precipitation to drainage headwaters. In contrast, where the canyon parallels the storm vector, storms can move quickly down into tributaries, impinging on canyon walls and directly affecting debris-flow source areas.

Standard morphometric measures of drainage-basin area and channel gradient are also significant and positively correlated with debris-flow

Table 4. Clay mineralogy of source material and debris flows in Grand Canyon[1]

Sample Type	Location (mile-side)	Illite[1] (weight %)	Kaolinite[1] (weight %)	Smectite[1] (weight %)	Other[1] (weight %)
Hermit Shale	7.9-L	54	41	0	5
Esplanade Sandstone					
- basal unit	20.5-R	50	40	2	8
Bright Angel Shale	58.0-L	68	22	0	10
Colluvium	24.4-L	29	62	0	9
Colluvium	58.0-L	20	68	0	12
Colluvium	62.2-R	32	35	7	26
Colluvium	62.5-R	43	40	8	9
Colluvium	62.6-R	22	49	2	27
Debris-flow deposit	62.6-R	58	24	0	18
Colluvium	63.3-R	49	23	10	18
Colluvium	67.2-L	10	82	0	8
Colluvium	68.5-L	22	57	0	21
Debris-flow deposit	71.2-R	19	31	0	50
Debris-flow deposit	72.0-R	48	30	0	22
Debris-flow deposit	75.5-L	62	17	0	21
Debris-flow deposit	98.2-R	42	38	0	20
Debris-flow deposit	126.9-L	43	43	2	12
Colluvium	127.3-L	44	25	17	14
Debris-flow deposit	127.5-L	38	38	0	24
Colluvium	127.6-L	45	29	6	20
Colluvium	179.4-L	35	29	6	30
Debris-flow deposit	179.4-L	34	38	4	24
Debris-flow deposit	205.5-L	56	15	8	21
Debris-flow deposit	224.5-L	60	15	6	19

[1] Minerals identified by semi-quantitative x-ray diffraction. Margin of area ± 20% (Starkey and others, 1984).

frequency. Larger drainages provide more source material and are more likely than smaller drainages to be hit by localized thunderstorms. Larger drainages also have more waterfalls and produce more runoff during widespread precipitation, especially those basins with large drainage areas above the canyon rim, such as Prospect Creek (river mile 179.4-L). Steep gradients maximize the transport energy of a given debris flow by minimizing travel distance and energy loss for a given potential energy of failure.

The positive correlation of debris-flow frequency with two variables that are inversely proportional to each other — drainage area and channel gradient — reflects the complexity of the debris-flow initiation process. Using the linear relation between drainage area and gradient (fig. 15), we calculated the relative ratio of the log odds of the two variables: -1:12. This ratio indicates that for a given increase in drainage-basin area, the odds of debris-flow reaching the river will increase but the channel gradient decreases, which results in a twelve-fold decrease in the same odds. Thus, although both area and channel gradient are statistically significant in the process of debris-flow initiation and transport, an increase in gradient has more impact than an increase in drainage area. This results, in part, from a non-linear relation between debris-flow frequency and drainage area; there is likely an optimal size of drainage area above which no additional debris flows are produced. Large tributaries produce as many debris flows as smaller tributaries, but fewer may reach the river as channel gradient and transport energy decrease.

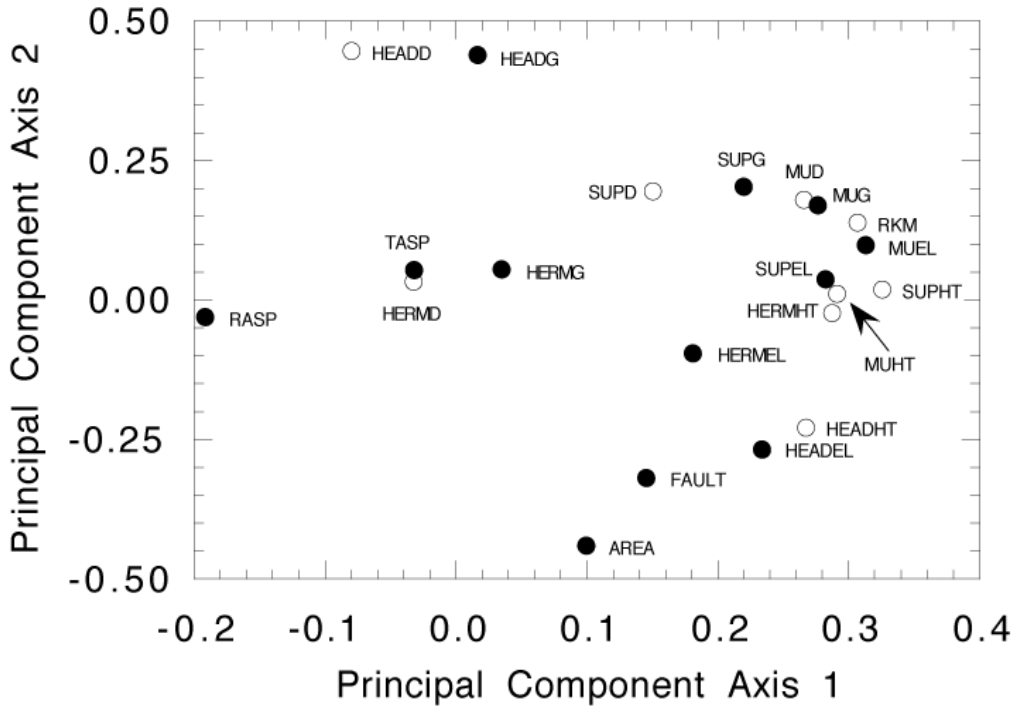

Figure 14. Graph showing the principal-component scores for variables used in the logistic regression model of eastern Grand Canyon. Variable names are given in table 4. Solid circles indicate variables that were retained for the logistic regression; open circles indicate variables that were removed from consideration in logistic regression.

The model for eastern Grand Canyon also contained a source-area component in the form of two measures of the Hermit Shale: its elevation and the channel gradient to its base. These variables reflect the dominant role of the Hermit Shale as the primary source of debris flows in eastern Grand Canyon. The presence of the gradient variable reinforces the importance of channel gradient in general to debris-flow transport. The selection of the elevation variable most likely has less to do with climatic effects than debris-flow energetics. The elevation variable is inversely related to debris-flow frequency, linking lower elevations of Hermit Shale to increased debris-flow occurrence. This relation likely is non-linear, with debris-flow frequency increasing with the elevation of shales to an optimum and then decreasing. As bedrock units rise higher above the river they also are farther away, increasing travel distance and energy dissipation. Eventually, energy loss over travel distance outweighs the gain in potential energy from increased height.

All elevation data for the Hermit Shale used in the eastern model have values greater than 100 m above river level. If even a small majority of these values lie above the hypothesized optimum, the linear relation between height and frequency fit by logistic regression would have the very slight negative slope calculated for the model. In contrast, the relation between elevation and debris-flow occurrence on the basis of precipitation should be strictly linear and positive within the range of elevations present in Grand Canyon.

Western Grand Canyon

A principal-component analysis of the drainage-basin data for western Grand Canyon indicated 9 redundant variables (fig. 16). As in eastern Grand Canyon, variables measuring height above and channel distance to river were eliminated in favor of elevation and gradient variables respectively. The remaining variables — the elevation and channel gradient to the Hermit Shale — were also highly correlated. When both variables were left in the data set, channel gradient to the Hermit Shale was selected as statistically significant. Removal of the elevation of the Hermit Shale had no effect on the model and so it was retained in the initial data set.

Backwards stepwise elimination with a significance threshold of 0.10 removed eight more variables as statistically insignificant (table 7). The overall model significance (ρ_m) is 0.18, indicating no significant difference between the final, five-variable and the original, thirteen variable model. The low value, however, suggests that the distinction between significant and insignificant variable is not as definite as in the eastern canyon. This decreased robustness is expected with the increased variability of a larger data set drawn from a diverse geographic area. Model accuracy in predicting observed debris-flow frequencies is 74 percent, with $\rho_C > 0.99$, indicating an excellent fit to the observed data. The verification data generated exactly the same group of significant variables, suggesting a robust model (table 8).

The significant variables selected for western Grand Canyon are drainage area, channel gradient, and variables representing the shales, which is similar to the model for eastern Grand Canyon. In western Grand Canyon, drainage area and channel gradient are inversely correlated with debris-flow frequency; smaller drainages and shallow gradients produce more debris flows. Using the linear relation between drainage area and channel gradient (fig. 17) the ratio of the log odds for area and gradient is -150:1. Thus, a given decrease in drainage area results in an increase in the odds of debris-flow occurrence that is 150 times greater than the decrease in odds resulting from the concurrent decrease in slope gradient. At face value, this relation is an inversion of the relation between area, gradient, and debris-flow frequency established in eastern Grand Canyon. However, considering the close correlation between drainage area and channel gradient (fig. 17), gradient and area may act as proxies for each other. In this case, an increase in drainage area in the west, represented in the model as a decrease in gradient, produces more debris flows. An increase in gradient, represented as a decrease in area, also produces more debris flows. This interpretation also maintains the dominant role of channel gradient on debris-flow frequency evident in the eastern canyon.

In western Grand Canyon, the primary debris-flow source area shifts from the Hermit Shale, which is at its highest elevation in the western canyon, to the Muav Limestone and its associated colluvial wedges. As in the model for eastern Grand Canyon, steeper gradients and low elevations are both selected for their role in debris-flow energy loss. The Hermit Shale, however, continues to be significant. Although it has risen to a fairly constant elevation since its appearance at river level in the eastern canyon, variations in drainage shape create variations in channel gradient to the Hermit Shale. Steep gradients to this important source area again correlate with increased debris-flow occurrence.

Non-significant Variables

River aspect, Θ, is notably absent from the list of statistically significant variables in western Grand Canyon. Because precipitation decreases across Grand Canyon from east to west, the impact of climatic effects on debris-flow frequency is likely to be weaker in the west than in the east. Also, regional structure is controlled by large fault systems in western Grand Canyon (for example, Huntoon and others, 1981). In general, most climatic variables were not selected as significant at either end of the canyon. Tributary aspect is clearly not as important as the overall aspect of the river in producing debris flows. Although many side tributaries have narrow, slick-rock bottoms, in general they open wide to the river, spreading out along the margins of the canyon. This is especially true at the height of debris-flow source areas. Only in the most constricted basins would tributary aspect control precipitation effects. Elevation variables were selected in both models, but they apparently serve as proxies for the energy of source failures instead of runoff-generating variables. Improved measures of climatic effects, such as direct measure of precipitation in the tributaries, may be more significantly related to debris-flow initiation.

The secondary role of the Supai Group as a debris-flow source lithology is indicated by the absence in both models of variables representing the Supai Group. This emphasizes the role of the Supai Group as a secondary producer of colluvium that accumulates downslope, rather than as a direct source of debris flows. The variable measuring total fault length in each basin was also not significant. Clearly, fault-derived source material is locally important in several drainages within Grand

Table 5. Calibration model for debris-flow frequency in tributaries of eastern Grand Canyon, Arizona

Drainage-basin variable	Variable Coefficient (β_v)	Wald Statistic (W)	Variable Significance[1] (ρ_v)	Log Odds (Ψ)	Model Significance (ρ_m)	Model Accuracy (α)	Goodness-of-fit Significance[2] (ρ_C)
Intercept	2.981	2.155	0.142	--	0.86	0.76	0.41
River aspect	3.246	9.889	0.002	25.7			
Log of drainage-basin area	2.192	4.124	0.042	9.0			
Log of channel gradient to Hermit Shale	0.955	3.565	0.059	2.6			
Log of channel gradient	3.558	3.048	0.801	35.1			
Elevation of Hermit Shale	-0.002	2.991	0.084	1.0			

Notes: Threshold of significance = 0.10; n = 78 observations.
[1] Based on a χ^2 distribution of the Wald statistic.
[2] Based on a χ^2 distribution of the Hosmer-Lemeshow goodness-of-fit statistic (C) with 8 degrees of freedom (Hosmer and Lemeshow, 1989).

Table 6. Verification model for debris-flow frequency in tributaries of eastern Grand Canyon, Arizona

Drainage-basin variable	Variable Coefficient (β_v)	Wald Statistic (W)	Variable Significance[1] (ρ_v)	Log Odds (Ψ)	Model Significance (ρ_m)	Model Accuracy (α)	Goodness-of-fit Significance[2] (ρ_C)
Intercept	2.199	1.726	0.189	--	0.70	0.72	0.70
River aspect	2.850	12.01	0.001	17.3			
Elevation of Hermit Shale	-0.001	3.42	0.064	1.0			
Log of channel gradient	2.891	2.917	0.088	18.0			
Log of drainage-basin area	1.345	2.593	0.107	3.8			
Log of channel gradient to Hermit Shale	0.614	2.416	0.120	18.0			

Notes: Threshold of significance = 0.10; n = 103 observations.
[1] Based on a χ^2 distribution of the Wald statistic.
[2] Based on a χ^2 distribution of the Hosmer-Lemeshow goodness-of-fit statistic (C) with 8 degrees of freedom (Hosmer and Lemeshow, 1989).

Table 7. Calibration model for debris-flow frequency in tributaries of western Grand Canyon, Arizona

Drainage-basin variable	Variable Coefficient (β_v)	Wald Statistic (W)	Variable Significance[1] (ρ_v)	Log Odds (Ψ)	Model Significance (ρ_m)	Model Accuracy (α)	Goodness-of-fit Significance[2] (ρ_C)
Intercept	3.367	4.450	0.035	n.a.	0.18	0.74	0.99
Log of drainage-basin area	-2.226	9.324	0.002	0.1			
Log of channel gradient to Hermit Shale	0.715	7.823	0.005	2.0			
Log of channel gradient	-5.221	7.144	0.007	0.01			
Elevation of Muav Limestone	-0.003	7.373	0.007	1.0			
Log of channel gradient to Muav Limestone	0.768	3.319	0.068	2.2			

Notes: Threshold of significance = 0.10; n = 86 observations.
[1] Based on a χ^2 distribution of the Wald statistic.
[2] Based on a χ^2 distribution of the Hosmer-Lemeshow goodness-of-fit statistic (C) with 8 degrees of freedom (Hosmer and Lemeshow, 1989).

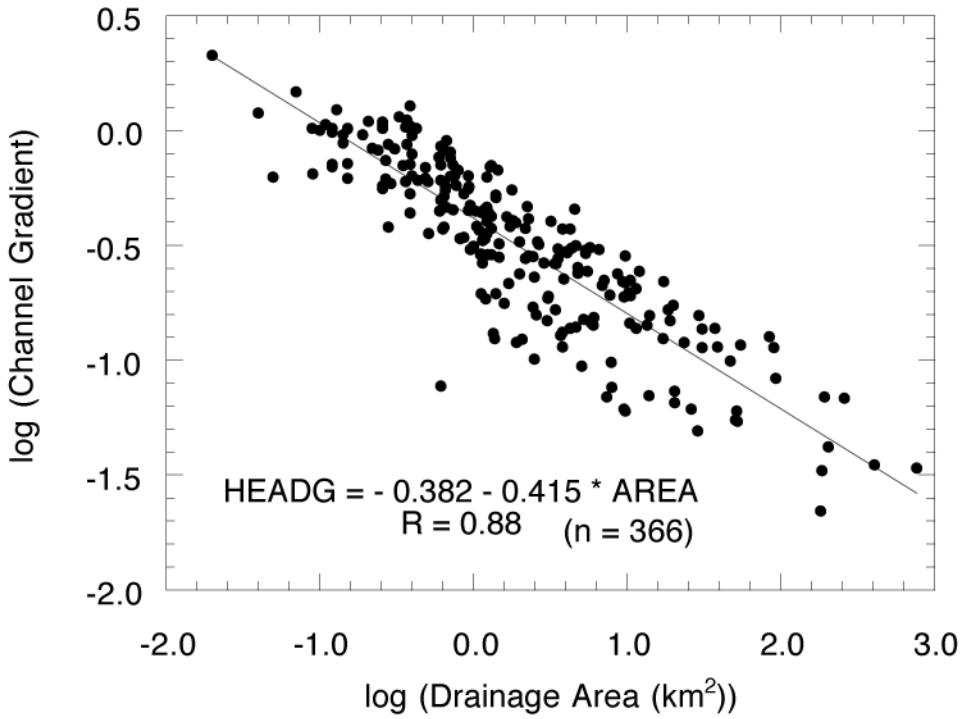

Figure 15. The relation between the log of the drainage-basin area and the log of the channel gradient for tributaries in eastern Grand Canyon. Variable names are given in table 4.

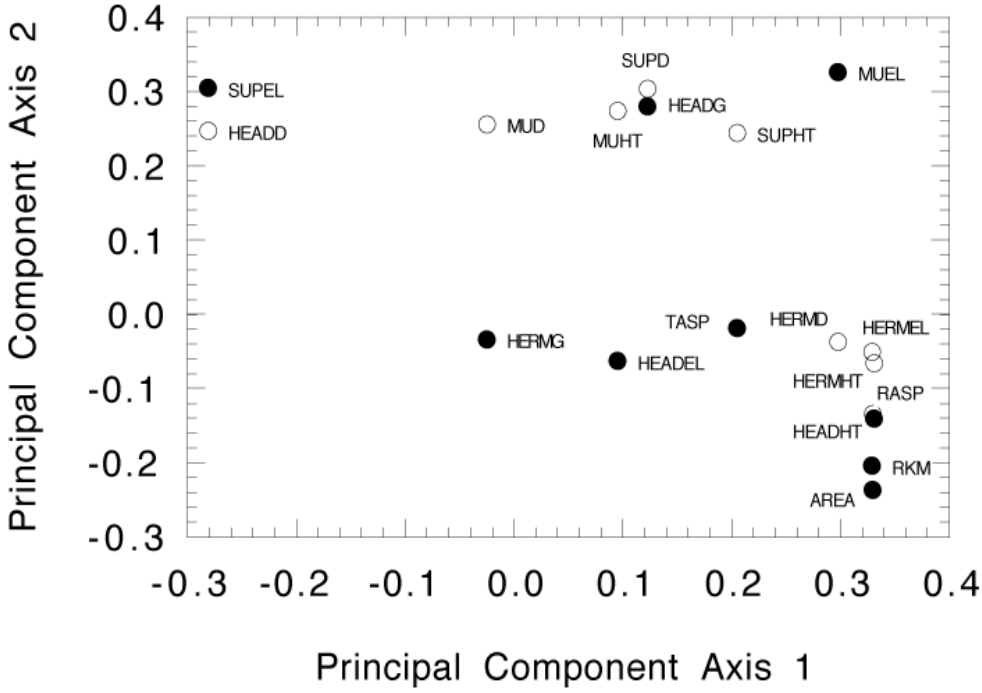

Figure 16. Graph showing the principal-component scores for variables used in the logistic regression model of western Grand Canyon. Variable names are given in table 4. Solid circles indicate variables that were retained for the logistic regression; open circles indicate variables that were removed from consideration in logistic regression.

Table 8. Verification model for debris-flow frequency in tributaries of western Grand Canyon, Arizona

Drainage-basin variable	Variable Coefficient (β_v)	Wald Statistic (W)	Variable Significance[1] (ρ_v)	Log Odds (Ψ)	Model Significance (ρ_m)	Model Accuracy (α)	Goodness-of-fit Significance[2] (ρ_C)
Intercept	1.774	1.924	0.165	n.a.	0.70	0.68	0.80
Log of drainage-basin area	-2.011	10.258	0.001	0.1			
Log of channel gradient	-4.632	8.289	0.004	0.01			
Log of channel gradient to Muav Limestone	0.737	5.404	0.020	2.1			
Elevation of Muav Limestone	-0.002	5.139	0.023	1.0			
Log of channel gradient to Hermit Shale	0.338	2.515	0.113	1.4			

Notes: Threshold of significance = 0.10; n = 111 observations.
[1] Based on a χ^2 distribution of the Wald statistic.
[2] Based on a χ^2 distribution of the Hosmer-Lemeshow goodness-of-fit statistic (C) with 8 degrees of freedom (Hosmer and Lemeshow, 1989).

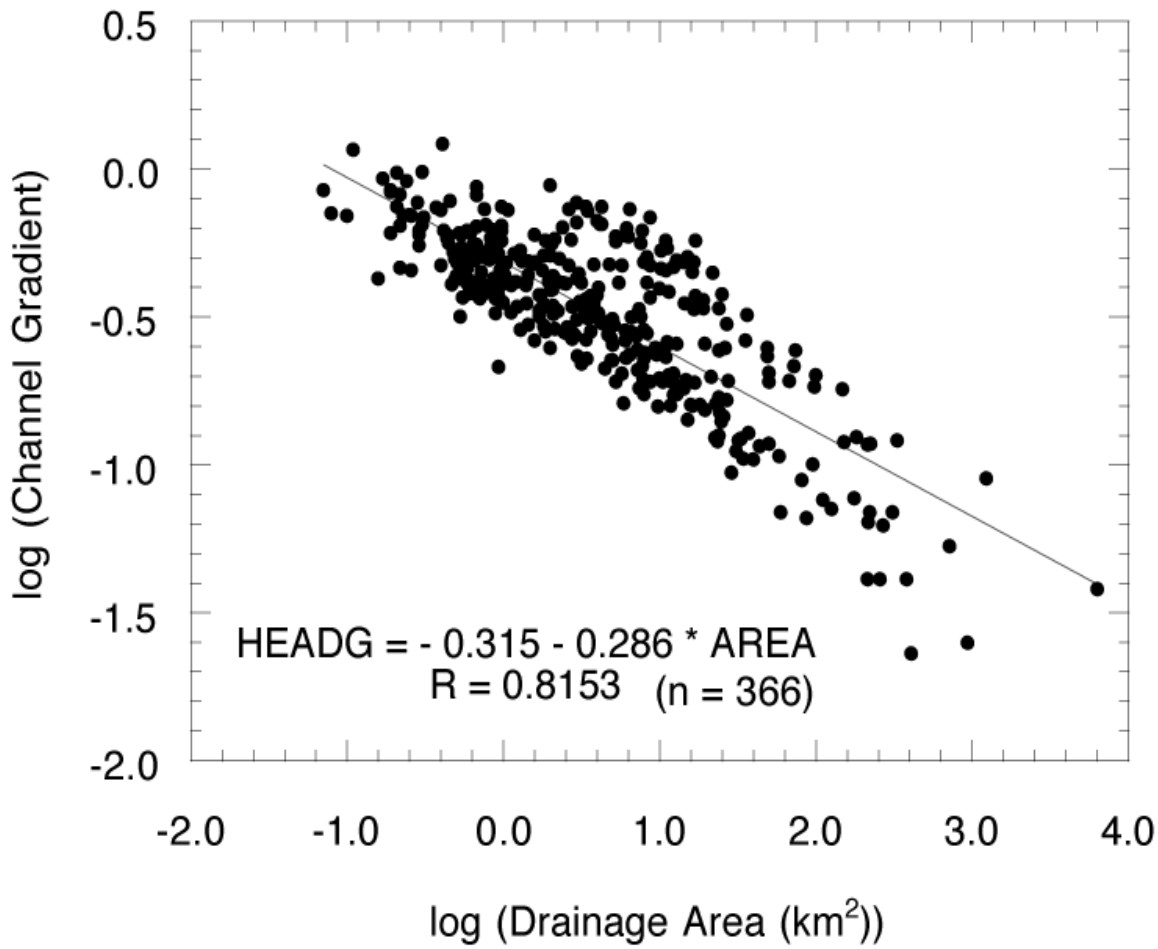

Figure 17. The relation between the log of the drainage-basin area and the log of the channel gradient for tributaries in western Grand Canyon. Variable names are given in table 4.

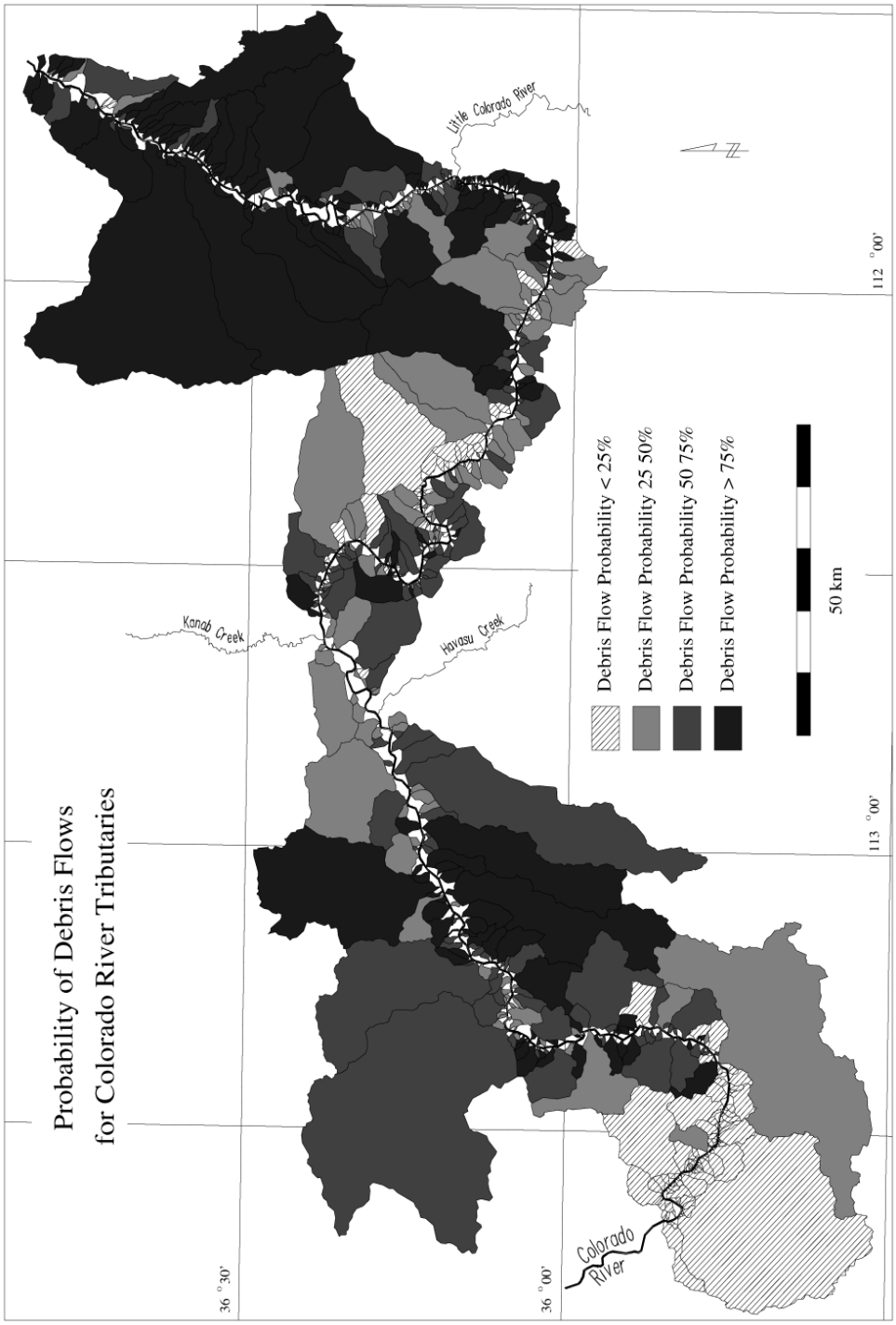

Figure 18. Map showing the probabilities of debris-flow occurrence during the last century in 600 tributaries of the Colorado River in Grand Canyon.

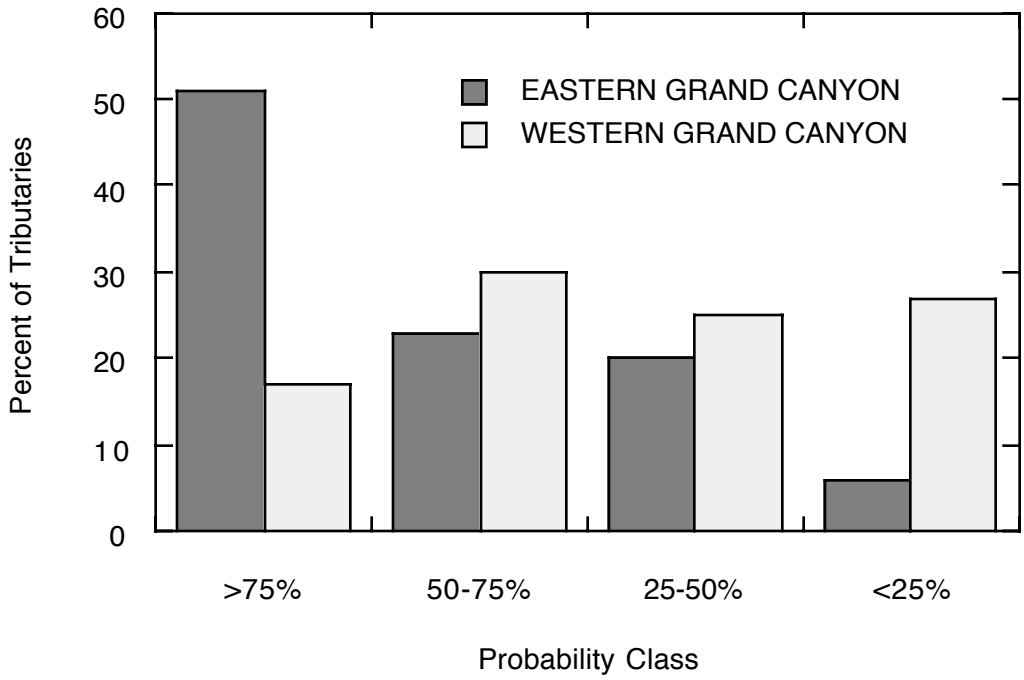

Figure 19. Histograms of the probability of debris-flow occurrence in eastern and western Grand Canyon.

Canyon, but it is not a primary contributor in the overall pattern of debris-flow probability. Although faults control the locations of tributaries (Dolan and others, 1978; Potochnik and Reynolds, 1990), the area and volume of fractured material produced by faulting does not appear to be important in initiating debris flows, except locally.

DISCUSSION AND CONCLUSIONS

Debris flows in Grand Canyon are one of the main controls on the geomorphic framework of the Colorado River, depositing large boulders that define the river's longitudinal profile. These mass movements are initiated when weathered bedrock or colluvial wedges fail during intense rainfall. These failures can be classified according to four failure mechanisms: 1) direct failure of weathered bedrock (12 percent); 2) failure of colluvium from the impact of runoff cascading from cliff pourovers, known as the "firehose effect" (36 percent); 3) failure of saturated colluvium (21 percent); and 4) combinations of these three mechanisms (30 percent).

A variety of geomorphic factors relating to climate, exposed lithologic strata, geologic structure, and drainage-basin morphology play various roles in the process of debris-flow initiation. Among these factors, the exposure of shale source areas at heights greater than 100 m above the mainstem is particularly critical in each of the four initiation mechanisms. Shales fail readily as weathered bedrock, produce abundant colluvial source material, and form slopes where colluvium collects. Shales also provide the fine particles and clay minerals (for example, kaolinite and illite) that appear to be essential to the stability of slurries, enabling debris flows to transport poorly-sorted sediments up to several kilometers from tributary sources to the Colorado River.

Earlier work has investigated the statistical significance of various morphometric variables in relation to flood magnitude, usually emphasizing drainage-basin area, mean-basin elevation, and amount or intensity of precipitation (Roeske, 1978; Thomas and others, 1994). Patton and Baker (1976) suggest that stream magnitude may also be a good predictor of flash-flood potential for small drainage basins. They argue that transient controls, such as climatic variability, also play a significant role. Shown (1970) includes all of these variables in modeling sediment transport in the southwest, as well as factors relating to surface geology and soils such as rock type, hardness, weathering, and texture.

Those drainage-basin variables that are most significant in influencing the binomial frequency of debris flows are well illustrated by a plot of the modeled probability of debris flows in all 600 geomorphically significant tributaries of Grand Canyon between Lees Ferry and Surprise Canyon (river miles 0-248; fig. 18). The results of the logistic regression model clearly demonstrate that debris flows in Grand Canyon do not occur randomly in space. The binomial frequency of debris flows is substantially higher in eastern Grand Canyon, where 51 percent of the tributaries have had a probability of debris flows greater than 75 percent during the last 100 years (fig. 19). In contrast, 17 percent of tributaries in western Grand Canyon have had a probability of debris flows greater than 75 percent. For all of Grand Canyon, 60 percent of the tributaries have had a debris-flow probability greater than 50 percent, although that probability was 74 percent in eastern Grand Canyon and 47 percent in western Grand Canyon.

Distinct patterns are evident in the debris-flow probability map, such as an overall higher probability of debris flows in eastern Grand Canyon (fig. 18). This is due to a combination of an increase in precipitation and a general trend in river aspect to the southwest that takes maximum advantage of increased precipitation. Also significant in eastern Grand Canyon is the presence of the Hermit Shale at an optimum height above the river. All three elements combine to make the stretch from Lees Ferry to 75-Mile Canyon the most prolific zone of debris-flow production in the Grand Canyon, as evidenced by the high probability of debris-flow occurrence (fig. 18).

These same trends also occur in western Grand Canyon. Debris flows fall off notably where the canyon turns to the north-west, perpendicular to the movement of severe storms. Although climatic variables were not selected as statistically significant in the models, they still seem to have an underlying influence. Debris-flow probability is lowest downstream from Diamond Creek, where precipitation is lowest and the river trends northwest. The results of the logistic regression model clearly demonstrate that variation in lithologic, morphometric, and climatic variables have a strong effect on the probability of debris flows in Grand Canyon.

REFERENCES CITED

Beverage, J.P., and Culbertson, J.K., 1964, Hyperconcentrations of suspended sediment: American Society of Civil Engineers, Journal of the Hydraulics Division, v. 90, p. 117-126.

Billingsley, G.H., and Elston, D.P., 1989, Geologic log of the Colorado River from Lees Ferry to Temple Bar, Lake Mead, Arizona, *in* Elston, D.P., Billingsley, G.H., and Young, R.A. (editors), Geology of Grand Canyon, northern Arizona: Washington, D.C., American Geophysical Union, p. 1-47.

Billingsley, G. H., Jr., and Huntoon, P.W., 1983, Geologic map of Vulcan's Throne and vicinity, western Grand Canyon: Grand Canyon Natural History Association, scale 1:48 000, 1 sheet.

Cooley, M.E., Aldridge, B.N., and Euler, R.C., 1977, Effects of the catastrophic flood of December, 1966, North Rim area, eastern Grand Canyon, Arizona: U.S. Geological Survey Professional Paper 980, 43 p.

Costa, J.E., and Wieczorek, G.F., 1987, Debris flows/avalanches: Process, recognition, and mitigation: Geological Society of America, Reviews in Engineering Geology, v. 7, 239 p.

Dolan, R., Howard, A., and Trimble, D., 1978, Structural control of the rapids and pools of the Colorado River in the Grand Canyon: Science, v. 202, p. 629-631.

Ford, T.D., Huntoon. P.W., Billingsley, G.H., Breed, W.J., 1974, Rock movement and mass wastage in the Grand Canyon, in Geology of the Grand

Canyon: Flagstaff, Museum of Northern Arizona, Grand Canyon Natural History Association Publication, p. 116-128.

Graf, W.L., 1979, Rapids in canyon rivers: Journal of Geology, v. 87, p. 533-551.

Graf, W.L., 1980, The effect of dam closure on downstream rapids: Water Resources Research, v. 16, p. 129-136.

Hamblin, W.K., and Rigby, J.K., 1968, Guidebook to the Colorado River, Part 1 — Lees Ferry to Phantom Ranch in Grand Canyon National Park: Provo, Utah, Brigham Young University Geology Studies, v. 15, part 5, 84 p.

Hampton, M.A., 1975, Competence of fine-grained debris flows: Journal of Sedimentary Petrology, v. 45, p. 834-844.

Hansen, E.M., and Shwarz, F.K., 1981, Meteorology of important rainstorms in the Colorado River and Great Basin drainages: National Weather Service Hydrometeorological Report No. 50, 167 p.

Haynes, D.D., and Hackman, R.J., 1978, Geology, structure, and uranium deposits of the Marble Canyon 1° x 2° quadrangle, Arizona: U.S. Geological Survey Miscellaneous Investigations Series Map I-1003, scale 1:250,000, 2 sheets.

Hereford, R., and Huntoon, P.W., 1990, Rock movement and mass wastage in the Grand Canyon, in Beus, S.S., and Morales, M. (editors), Grand Canyon geology: New York, Oxford University Press, p. 443-459.

Hereford, R., Thompson, K.S., Burke, K.J., and Fairley, H.C., 1996, Tributary debris fans and the late Holocene alluvial chronology of the Colorado River, eastern Grand Canyon, Arizona: Geological Society of America Bulletin, v. 108, p. 3-19.

Hirschboeck, K.K., 1985, Hydroclimatology of flow events in the Gila River Basin, central and southern Arizona [Ph.D. dissertation.]: Tucson, Arizona, University of Arizona, 335 p.

Hosmer, D.W., and Lemeshow, S., 1989, Applied logistic regression: New York, John Wiley and Sons, 307 p.

Howard, A., and Dolan, R., 1981, Geomorphology of the Colorado River in Grand Canyon: Journal of Geology, v. 89, p. 269-297.

Huntoon, P.W., and Billingsley, G.H., 1983, Geologic map of Vulcan's Throne and vicinity, western Grand Canyon, Arizona: Grand Canyon Natural History Association, scale 1:48 000, 1 sheet.

Huntoon, P.W., Billingsley, G.H., and Clark, M.D., 1981, Geologic map of the Hurricane Fault Zone and vicinity, western Grand Canyon, Arizona: Grand Canyon Natural History Association, scale 1:48 000, 1 sheet.

Huntoon, P.W., Billingsley, G.H., Breed, W.J., Sears, W.J., Ford, T.D., Clark, M.D., Babcock, S., and Brown, E.H., 1986, Geologic map of the eastern part of the Grand Canyon National Park, Arizona: Grand Canyon Natural History Association Map, scale 1:62,500, 1 sheet.

Johnson, A.M., and Rodine, J.R., 1984, Debris flow, *in* Brunsden, D., and Prior, D.B. (editors), Slope instability: New York, John Wiley and Sons, p. 257-361.

Kieffer, S.W., 1985, The 1983 hydraulic jump in Crystal Rapid — Implications for river running and geomorphic evolution in the Grand Canyon: Journal of Geology, v. 93, p. 385-406.

Leopold, L.B., 1969, The rapids and pools — Grand Canyon, *in* The Colorado River Region and John Wesley Powell: U.S. Geological Survey Professional Paper 669, p. 131-145.

Major, J.J., and Pierson, T.C., 1992, Debris flow rheology: Experimental analysis of fine grained slurries: Water Resources Research, v. 28, no. 3, p. 841-858.

Melis, T.S., and Webb, R.H., 1993, Debris flows in Grand Canyon National Park, Arizona — Magnitude, frequency and effects on the Colorado River, *in* Shen, H.W., Su, S.T., and Wen, F. (editors), Hydraulic Engineering '93: New York, American Society of Civil Engineers, Proceedings of the ASCE Conference, San Francisco, California, p. 1290-1295.

Melis, T.S., Webb, R.H., Griffiths, P.G., and Wise, T.J., 1994, Magnitude and frequency data for historic debris flows in Grand Canyon National Park and vicinity, Arizona: U.S. Geological Survey Water-Resources Investigations Report 94-4214, 285 p.

National Oceanic and Atmospheric Administration (NOAA), 1996, Climatological data, Arizona, February 1996: Asheville, North Carolina, Climatic Data Center, v. 100, no. 2, 36 p.

Patton, P.C., and Baker, V.R., 1976, Morphometry and floods in small drainage basins subject to diverse hydrogeomorphic controls: Water Resources Research, v. 12, p. 941-952.

Pierson, T.C., and Costa, J.E., 1987, A rheologic classification of subaerial sediment-water flows, *in* Costa, J.E., and Wieczorek, G.F. (editors), Debris flows / avalanches — Process, recognition, and mitigation: Reviews in Engineering Geology, v. 7, p. 1-12.

Potochnik, A.R., and Reynolds, S.J., 1990, Side canyons of the Colorado River, Grand Canyon, *in* Beus, S.S., and Morales, M. (editors), Grand Canyon geology: New York, Oxford University Press, p. 461-481.

Powell, J.W., 1875, Exploration of the Colorado River and its canyons: New York, Dover Publications, 400 p.

Rodine, J.D., and Johnson, A.R., 1976, The ability of debris, heavily freighted with coarse clastic materials, to flow on gentle slopes: Sedimentology, v. 23, p. 213-234.

Roeske, R.H., 1978, Methods for estimating the magnitude and frequency of floods in Arizona: Arizona Department of Transportation Final Report ADOT-RS-15(121), 82 p.

SAS, 1990, SAS/STAT User's Guide, Version 6, Fourth Edition, Volume 2: Cary, North Carolina, SAS Institute, Incorporated, 846 p.

Savage, S.B., and Hutter, K., 1987, The motion of a finite mass of granular material down a rough incline: Journal of Fluid Mechanics, v. 199, p. 177-215.

Schmidt, J.C., Grams, P.E., and Webb, R.H., 1995, Comparison of the magnitude of erosion along two large regulated rivers: Water Resources Bulletin, v. 31, p. 617-631.

Sellers, W.D., Hill, R.H., and Sanderson-Rae, M. (editors), 1985, Arizona climate: Tucson, University of Arizona Press, 143 p.

Shown, L.M., 1970, Evaluation of a method for estimating sediment yield: U.S. Geological Survey Professional Paper 700-B, p. B245-B299.

Smith, W., 1986, The effects of eastern North Pacific tropical cyclones on the southwestern United States: Salt Lake City, Utah, National Oceanic and Atmospheric Administration, Technical Memorandum NWS-WR-197, 229 p.

Starkey, H.C., Blackmoun, P.D., Hauff, P.L., 1984, The routine mineralogical analysis of clay-bearing samples: U.S. Geological Survey Bulletin 1563, 32 p.

Stephens, H.G., and Shoemaker, E.M., 1987, In the footsteps of John Wesley Powell: Boulder, Colorado, Johnson Books, 286 p.

Stevens, L., 1990, The Colorado River in Grand Canyon, A guide: Flagstaff, Arizona, Red Lake Books, 107 p.

Thomas, B.E., Hjalmarson, H.W., and Waltemeyer, S.D., 1994, Methods for estimating the magnitude and frequency of floods in southwestern United States: U.S. Geological Survey Open-File Report 93-419, 219 p.

Turner, R.M., and Karpiscak, M.M., 1980, Recent vegetation changes along the Colorado River between Glen Canyon Dam and Lake Mead, Arizona: U.S. Geological Survey Professional Paper 1132, 125 p.

U.S. Department of Commerce, 1966, Arizona, Hourly precipitation data, December 1966: U.S. Department of Commerce, Environmental Science Services Administration, v. 16, no. 12, 5 p.

U.S. Department of Interior, 1995, Operation of Glen Canyon Dam, Final environmental impact statement: Salt Lake City, Utah, Bureau of Reclamation, 337 p. + appendices.

U.S. Water Resources Council, 1981, Guidelines for determining flood flow frequency: Hydrology Subcommittee Bulletin 17B, 183 p.

Webb, R.H., 1996, Grand Canyon, a century of environmental change: Tucson, University of Arizona Press, 290 p.

Webb, R.H., and Betancourt, J.L., 1992, Climatic variability and flood frequency of the Santa Cruz River, Pima County, Arizona: U.S. Geological Survey Water-Supply Paper 2379, 40 p.

Webb, R.H., and Melis, T.S., 1995, The 1995 debris flow at Lava Falls Rapid: Nature Notes, v. 11, p. 1-4.

Webb, R.H., Pringle, P.T., Reneau, S.L., and Rink, G.R., 1988, Monument Creek debris flow, 1984 — Implications for formation of rapids on the Colorado River in Grand Canyon National Park: Geology, v. 16, p. 50-54.

Webb, R.H., Pringle, P.T., and Rink, G.R., 1989, Debris flows in tributaries of the Colorado River in Grand Canyon National Park, Arizona: U.S. Geological Survey Professional Paper 1492, 39 p.

Webb, R.H., Melis, T.S., Wise, T.W., and Elliott, J.G., 1996, "The Great Cataract," The effects of late Holocene debris flows on Lava Falls Rapid, Grand Canyon National Park, Arizona: U.S. Geological Survey Open-file Report 96-460, 96 p.